Robotica (2021), **39**, pp. 2306–2332
doi:10.1017/S0263574721000333

CAMBRIDGE UNIVERSITY PRESS

RESEARCH ARTICLE

Global inverse optimal exponential path-tracking control of mobile robots driven by Lévy processes

K. D. Do

School of Civil and Mechanical Engineering, Curtin University, Bentley, WA 6102, Australia
Email: duc@curtin.edu.au

Received: 16 October 2019; **Revised:** 5 March 2021; **Accepted:** 9 March 2021; **First published online:** 19 April 2021

Keywords: Mobile robot, Path-tracking, Inverse optimality, Exponential stability, Lévy processes

Abstract

This paper formulates and solves a new problem of global practical inverse optimal exponential path-tracking control of mobile robots driven by Lévy processes with unknown characteristics. The control design is based on a new inverse optimal control design for nonlinear systems driven by Lévy processes and ensures global practical exponential stability almost surely and in the pth moment for the path-tracking errors. Moreover, it minimizes cost function that penalizes tracking errors and control torques without having to solve a Hamilton–Jacobi–Bellman or Hamilton–Jaccobi–Isaacs equation.

1. Introduction

Wheeled mobile robots subject to nonholonomic constraints have a wide range of applications. Their control receives extensive attention from both control and robotic communities, see refs. [1, 2, 3, 4] and references therein for an introduction to this expanding area. Excellent control results have been obtained. Due to their nonholonomic constraints, see ref. [5] (hence, no stationary continuous state feedback controller can stabilize them), the results on control of mobile robots are often classified into stabilization (where either time-varying or discontinuous controllers were designed, see for example refs. [6, 7, 8, 9, 10]), trajectory-tracking (where the mobile robots must track reference positions, orientation, and time, see for example refs. [9, 10, 11, 12, 13]), path-following (where the mobile robots must move on a reference path with a desired velocity, see refs. [6, 14, 15, 16]), and path-tracking (an interlaced objective between trajectory-tracking and path-following, where the mobile robots must track a reference path but without tracking time, see refs. [17, 18, 19, 20, 21, 22, 23]). In the above works, Lyapunov's direct method in ref. [24] and backstepping technique in ref. [25] are often used, where the orientation (heading angle) is usually considered as an immediate control to control the positions of the mobile robots to overcome the difficulty due to the fact that the sway axis is unactuated. There are several issues with the above works. First, dynamics of the mobile robots either ignore external disturbances or include deterministic disturbances. Second, when tracking/following a straight line (a linear reference trajectory or linear path), only (global) weak asymptotic stability (see ref. [26] for a definition of weak and strong asymptotic stability) is achieved. Third, the control design is not optimal in the sense that no meaningful cost function (that penalizes both tracking/following errors and control inputs) is minimized. The aim of this paper is to relax the above limitations.

Most dynamical systems including wheeled mobile robots are subject to complex external disturbances, which can be modeled by Lévy processes because they can be decomposed to drifts (deterministic), diffusions, and jumps thanks to the Itô–Lévy decomposition, see ref. [27]. While excellent and extensive control design results are available for systems driven by diffusions (in refs. [28, 29, 30, 31, 32], there are a few recent works on control of systems driven by Lévy processes

© The Author(s), 2021. Published by Cambridge University Press.

https://doi.org/10.1017/S0263574721000333 Published online by Cambridge University Press

(in refs. [33, 34, 35, 36, 37, 38, 39]). This is mainly due to difficulties in handling an extra term due to the random jumps in the infinite generator of a Lyapunov function candidate in addition to the Hessian term, which only appears in a system driven by diffusions.

When controlling a dynamical system, in addition to fulfillment of a control objective, control effort should not be unnecessarily wasted and the control gain margin should be as large as desirable. These are achieved by an optimal control design in ref. [40]. However, (direct) optimal control of nonlinear systems was abandoned because solving Hamilton–Jaccobi–Bellman (HJB) or Hamilton–Jaccobi–Isaacs (HJI) equations is a formidable task. The inverse optimal control approach in refs. [40, 41] relaxes the above task, where the cost functional is specified by the designer rather than being pre-specified. While inverse optimal control of stochastic systems driven by diffusions was considered with excellent results (in refs. [28, 29, 41, 42]), it is only recently considered for stochastic systems driven by Lévy processes in ref. [43], where the Lévy processes exclude a drift term and the auxiliary system used for inverse optimal control design with gain assignment is required to be global exponential stable (either almost sure (a.s.) or in the pth moment). This paper proposes a new inverse optimal control design result that relaxes the above limitations. The main contributions of this paper are threefold as follows.

First, the optimal control problem that forces a mobile robot subject to complex disturbances modeled by Lévy processes to track a reference path is formulated as minimizing worst case risk in the risk-sensitive theory, see Control Objective 2.2 and Remark 2.2. The cost function penalizes the tracking errors, control torques provided by motors, and external disturbances. This formulation allows us to solve the optimal tracking control problem without having to solve a HJI equation.

Second, a new theorem (Theorem 3.2) is developed to design inverse optimal gain assignment stabilizers for nonlinear systems driven by Lévy processes with unknown noise characteristics. This theorem utilizes Theorem 3.1, which is a generalized version of Theorem 2.1 in ref. [39] to handle a persistency excitation (PE) condition in the infinitesimal generator of the Lyapunov function, to develop a control design method that minimizes a cost function penalizing states, control, and disturbances without having to solve a HJI equation. The control Lyapunov function is a solution to a family of HJI equations. Arbitrary disturbance attenuation can be achieved. In addition, the proposed inverse optimal stabilizers have an infinite gain margin. In comparison with the recent work in ref. [43], Theorem 3.2 allows unknown drifts in the Lévy processes and practical exponential stability of the auxiliary system.

Third, guided by Theorem 3.1, a new inverse optimal path-tracking controller is designed for mobile robots subject to external disturbances modeled by Lévy processes summarized in Theorem 4.1. In the design, the robot dynamics are directly considered (without a coordinate transformation as in existing works). The main ingredients used in the control design include a special design of the rate of the path parameter of the reference path, which results in global (practical) exponential stability of the tracking errors both a.s. and in the pth moment, quartic Lyapunov functions, and Theorem 3.2.

In comparison with the existing works on controlling mobile robots, the inverse optimal control design for mobile robots in this paper has three distinct features. First, external disturbances are allowed to be complex as they are modeled by Lévy processes. Second, the control design achieves global exponential stability of the tracking errors both a.s. and in the pth moment. This is much more desirable than either global weak or strong asymptotic stability in the sense that while global exponential stability is usually robust to arbitrarily large input disturbances, global weak asymptotic stability can only be robust to small input disturbances and global strong asymptotic stability does not result in a fast convergence when the states are in the neighborhood of the origin. Third, the control design yields a tracking controller that has an infinite gain margin and minimizes a cost function. This cost function puts appropriate penalty on tracking errors, control torques, and disturbances.

Notations. The symbols $\wedge$ and $\vee$ denote the infimum and supremum operators, respectively. The symbol $\mathbb{E}$ denotes the expected value.

https://doi.org/10.1017/S0263574721000333 Published online by Cambridge University Press

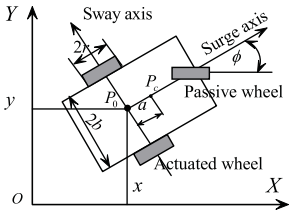


Figure 1. *Robot parameters.*

2. Problem statement

2.1. Robot dynamics

We consider a unicycle-type mobile robot with no wheel slips, see Fig. 1 where each actuated wheel is driven by a motor (to provide control torque), while the passive wheel is added for safety. This robot has the following dynamics, see ref. [44]:

$$\begin{aligned}
\dot{x} &= \frac{r}{2}(\omega_1 + \omega_2)\cos(\phi),\\
\dot{y} &= \frac{r}{2}(\omega_1 + \omega_2)\sin(\phi),\\
\dot{\phi} &= \frac{r}{2b}(\omega_1 - \omega_2),\\
\boldsymbol{M}\dot{\boldsymbol{\omega}} &= -\boldsymbol{C}(\omega_1 - \omega_2)\boldsymbol{\omega} - \boldsymbol{D}\boldsymbol{\omega} + \boldsymbol{\tau} + \boldsymbol{\Xi},
\end{aligned} \tag{1}$$

where (x, y) denotes the position, that is, the coordinates of the middle point, P_0, between the left and right driving wheels, and ϕ denotes the heading angle of the robot coordinated in the earth-fixed frame OXY, see Fig. 1, $\boldsymbol{\omega} = [\omega_1 \ \ \omega_2]^T$ with ω_1 and ω_2 being the angular velocities of the wheels of the robot, $\boldsymbol{\tau} = [\tau_1 \ \ \tau_2]^T$ with τ_1 and τ_2 being the control torques applied to the wheels of the robot. The mass matrix $\boldsymbol{M}$, skew-symmetric matrix $\boldsymbol{C}$, and damping matrix $\boldsymbol{D}$ in (1) are given by

$$\boldsymbol{M} = \begin{bmatrix} m_{11} & m_{12} \\ m_{12} & m_{11} \end{bmatrix}, \ \boldsymbol{C} = \frac{rc}{2b}\begin{bmatrix} 0 & 1 \\ -1 & 0 \end{bmatrix}, \ \boldsymbol{D} = \begin{bmatrix} d_{11} & 0 \\ 0 & d_{22} \end{bmatrix} \tag{2}$$

with

$$\begin{aligned}
&c = \frac{1}{2b}r^2 m_c a, \ \ m_{11} = \frac{1}{4b^2}r^2(mb^2 + I) + I_w, \ \ \ m_{12} = \frac{1}{4b^2}r^2(mb^2 - I),\\
&m = m_c + 2m_w, \ \ I = m_c a^2 + 2m_w b^2 + I_c + 2I_m,
\end{aligned} \tag{3}$$

where m_c and m_w are the masses of the body and wheel with a motor, respectively; I_c, I_w, and I_m are the moments of inertia of the body about the vertical axis through P_c (center of mass), the wheel with the rotor of a motor about the wheel axis, and the wheel with the rotor of a motor about the wheel diameter, respectively; r, a, and b are defined in Fig. 1; the nonnegative constants d_{11} and d_{22} are the damping coefficients; $\boldsymbol{\Xi}$ denotes the disturbance vector. The disturbance vector $\boldsymbol{\Xi}$ enters at the torque level rather than at the velocity level as in refs. [29, 45, 46, 47] to reflect the external moments induced by external objects. In this paper, we use the stochastic treatment with Lévy processes (rather than deterministic and probabilistic [48]) because they can cover a number of important processes such as Wiener process (or Brownian motion), Poisson process, stable and self-decomposable processes and subordinators, see ref. [27]. For example, the robot can be exposed to a bombard of surrounding objects, which result in jerk noise modeled as the sum of independent random variables hitting the agents at Poisson times.

https://doi.org/10.1017/S0263574721000333 Published online by Cambridge University Press

Jerk noise is a Lévy process (a process with stationary independent increments) and is a natural non-Gaussian generalization of white Gaussian noise. Therefore, we model $\boldsymbol{\Xi}$ as Lévy processes, which can be decomposed into drifts (deterministic), diffusions, and jumps due to the Itô–Lévy decomposition, see ref. [27]:

$$\boldsymbol{\Xi} = \boldsymbol{\theta}_0(t) + \boldsymbol{\Theta}_1(t)\frac{d\boldsymbol{W}(t)}{dt} + \sum_{j=1}^{m_2} \boldsymbol{\Phi}^{(j)}(t) \int_{|\xi_j|<\varepsilon_j} \frac{d\widetilde{N}_j(dt, d\xi_j)}{dt}, \tag{4}$$

Each term in the above expression is explained as follows. The term $\boldsymbol{\theta}_0(t)$ denotes the unknown (but bounded) deterministic disturbance. The term $\boldsymbol{\Theta}_1(t)\frac{d\boldsymbol{W}(t)}{dt}$ denotes the stochastic diffusion disturbance with $\boldsymbol{\Theta}_1$ being an unknown (but bounded) covariance matrix of the Wiener process vector $\boldsymbol{W}(t)$. The term $\sum_{j=1}^{m_2} \boldsymbol{\Phi}^{(j)}(t) \int_{|\xi_j|<\varepsilon_j} \frac{d\widetilde{N}_j(dt,d\xi_j)}{dt}$ with $m_2 \geq 1$ and $\varepsilon_j > 0$ denotes the stochastic jump vector with $\boldsymbol{\Phi}^{(j)}(t)$ being an unknown matrix and $\widetilde{N}_j(dt, d\xi_j) = N_j(dt, d\xi_j) - dt\nu(d\xi_j)$, where $N_j(dt, d\xi_j)$ is the j^{th} Poisson random measure and $\nu(d\xi_j)$ is the jth intensity measure. See Section 3 for more details.

Substituting (4) into (1) yields the stochastic dynamics of the mobile robot:

$$\begin{aligned}
dx &= \frac{r}{2}(\omega_1 + \omega_2)\cos(\phi)dt,\\
dy &= \frac{r}{2}(\omega_1 + \omega_2)\sin(\phi)dt,\\
d\phi &= \frac{r}{2b}(\omega_1 - \omega_2)dt,\\
\boldsymbol{M}d\boldsymbol{\omega} &= \big[-\boldsymbol{C}(\omega_1 - \omega_2)\boldsymbol{\omega} - \boldsymbol{D}\boldsymbol{\omega} + \boldsymbol{\tau} + \boldsymbol{\theta}_0(t)\big]dt + \boldsymbol{\Theta}_1(t)d\boldsymbol{W}(t) + \sum_{j=1}^{m_2} \boldsymbol{\Phi}^{(j)}(t) \int_{|\xi_j|<\varepsilon_j} d\widetilde{N}_j(dt, d\xi_j).
\end{aligned} \tag{5}$$

2.2. Control objective

In this paper, we address the following exponential and inverse optimal path-tracking control objective:

Control Objective 2.1. Assume that the reference path $(x_d(s), y_d(s))$, with s being the path parameter, is non-singular, that is, there exists a strictly positive constant ε_1 such that

$$x_d'^2(s) + y_d'^2(s) \geq \varepsilon_1, \tag{6}$$

where $x_d'(s) = \frac{\partial x_d}{\partial s}$ and $y_d'(s) = \frac{\partial y_d}{\partial s}$. The desired rate $\dot{s}_d$ of the reference path parameter is smooth and bounded and satisfies the PE condition:

$$\int_{t_0}^{t} (\dot{s}_d(\tau))^2 d\tau \geq \varepsilon_2(t - t_0), \tag{7}$$

where ε_2 is a strictly positive constant. The reference heading angle ϕ_d is defined as:

$$\phi_d(s(t)) = \arcsin\left(\frac{y_d'(s(t))}{\sqrt{x_d'^2(s(t)) + y_d'^2(s(t))}}\right). \tag{8}$$

Under the above assumptions, design the control input vector $\boldsymbol{\tau}$ to achieve two desired properties:

(1) Global practical exponential stability in the pth moment, a.s., and in probability of the tracking errors $(x - x_d, y - y_d, \phi - \phi_d)$.

https://doi.org/10.1017/S0263574721000333 Published online by Cambridge University Press

(2) A cost function penalizing both the tracking errors and the control effort. Specifically, this cost function is of the form:

$$J(\boldsymbol{\tau}_e) = \sup_{\mathcal{D}} \left(\lim_{t\to\infty} \sup \mathbb{E} \left\{ S\left(\boldsymbol{X}_e(t), t\right) + \int_{t_0}^{t} \left[\varphi\left(\boldsymbol{X}_e, r\right) + \hat{\gamma}_2 \left(\left\| \boldsymbol{R}_2^{\frac{1}{2}}\left(\boldsymbol{X}_e, r\right) \boldsymbol{\tau}_e \right\| \right) - \hat{\gamma}_0 \left(\|\boldsymbol{\theta}_0\| \right) \right.\right.\right.$$

$$\left.\left.\left. - \hat{\gamma}_1 \left(\|\boldsymbol{\Theta}_1 \boldsymbol{\Theta}_1^T\| \right) - \sum_{j=1}^{m_2} \hat{\gamma}_{3j}\left(\varpi_j\right) \right] dr \right\} \right), \tag{9}$$

where $\mathcal{D} := (\boldsymbol{\theta}_0, \boldsymbol{\Theta}_1, \boldsymbol{\varpi}) \in \mathcal{D}_0 \times \mathcal{D}_1 \times \mathcal{D}_2$ with $\mathcal{D}_i, i = 0, 1, 2$ being bounded sets, which the unknown Lévy characteristics (i.e., the drift $\boldsymbol{\theta}_0$, the covariance matrix $\boldsymbol{\Theta}_1$, and the intensity measure $\boldsymbol{\varpi} := \text{col}(\varpi_1, \cdots, \varpi_{m_2})$ with $\varpi_j := \int_{|\xi_j|<\varepsilon_j} \nu_j(d\xi_j)$) belong to; $\boldsymbol{X}_e$ denotes the tracking error vector; $\boldsymbol{\tau}_e = \boldsymbol{\tau} - \boldsymbol{\tau}_d$ with $\boldsymbol{\tau}_d$ being the reference torque input, that is,

$$\boldsymbol{\tau}_d = \boldsymbol{C}(\omega_{1d} - \omega_{2d})\boldsymbol{\omega}_d + \boldsymbol{D}\boldsymbol{\omega}_d + \boldsymbol{M}\dot{\boldsymbol{\omega}}_d, \tag{10}$$

with $\boldsymbol{\omega}_d = [\omega_{1d} \ \omega_{2d}]^T$ being the reference angular velocities of the wheels; S is a positive definite function; φ is a positive definite function for all $t \geq t_0 \geq 0$ and $\|\boldsymbol{X}_e\| \geq \delta$ with $\delta \geq 0$ being a positive constant; $\boldsymbol{R}_2$ is a positive definite matrix; and $\hat{\gamma}_i, i = 0, 1, 2, 3j$ are class $\mathcal{K}_\infty$-functions, whose derivative $\hat{\gamma}_i' := \frac{d\hat{\gamma}_i(r)}{dr}$ is also a class $\mathcal{K}_\infty$-function.

This control objective deserves the following discussions.

Remark 2.1. The PE condition (7) implies that we are solving a path-tracking control problem (not a stabilization problem) and that the robot allows to forward tracking (for the case $\dot{s}_d > 0$), backward tracking (for the case $\dot{s}_d < 0$), and repeat of forward and backward tracking ($\dot{s}_d$ is both positive and negative such as $\dot{s}_d = \sin(t)$). Moreover, the reference path (x_d, y_d) can be a curve or a straight line or a combination of both. A simple calculation shows that

$$\begin{aligned} \dot{x}_d &= \cos(\phi_d)\bar{u}_d\dot{s}, \\ \dot{y}_d &= \sin(\phi_d)\bar{u}_d\dot{s}, \end{aligned} \tag{11}$$

where $\bar{u}_d = \sqrt{x_d'^2 + y_d'^2}$.

Remark 2.2. In the risk-sensitive theory, the cost function (9) refers to as minimizing worst case risk. This cost function is elaborated as follows. Let δ be a nonnegative constant. Define the set

$$\begin{aligned} \mathcal{A} = \left\{ \left(\|\boldsymbol{X}_e\| \geq \delta\right) \cap \left(\varphi\left(\boldsymbol{X}_e, t\right) + \hat{\gamma}_2 \left(\left\| \boldsymbol{R}_2^{\frac{1}{2}}\left(\boldsymbol{X}_e, t\right) \boldsymbol{\tau}_e \right\| \right) \right.\right. \\ \left.\left. \geq \sup_{\mathcal{D}} \left(\hat{\gamma}_0\left(\|\boldsymbol{\theta}_0\|\right) + \hat{\gamma}_1\left(\|\boldsymbol{\Theta}_1\boldsymbol{\Theta}_1^T\|\right) + \sum_{j=1}^{m_2} \hat{\gamma}_{3j}\left(\varpi_j\right) \right) \right) \right\}. \end{aligned} \tag{12}$$

We consider two cases: inside of the set $\mathcal{A}$ and outside of the set $\mathcal{A}$.

(1) Inside of the set $\mathcal{A}$: In this case, $J(\boldsymbol{\tau}_e)$ is positive definite. We rewrite (9) as follows:

$$\begin{aligned} &\sup_{\mathcal{D}} \left(\lim_{t\to\infty} \sup \mathbb{E} \left\{ \int_{t_0}^{t} \left[\hat{\gamma}_0\left(\|\boldsymbol{\theta}_0\|\right) + \hat{\gamma}_1\left(\|\boldsymbol{\Theta}_1\boldsymbol{\Theta}_1^T\|\right) + \sum_{j=1}^{m_2} \hat{\gamma}_{3j}\left(\varpi_j\right) \right] dr \right\} \right) + J\left(\boldsymbol{\tau}_e\right) \\ &= \lim_{t\to\infty} \sup \mathbb{E} \left\{ S\left(\boldsymbol{X}_e\left(t\right), t\right) + \int_{t_0}^{t} \left[\varphi\left(\boldsymbol{X}_e, r\right) + \hat{\gamma}_2 \left(\left\| \boldsymbol{R}_2^{\frac{1}{2}}\left(\boldsymbol{X}_e, r\right) \boldsymbol{\tau}_e \right\| \right) \right] dr \right\} \ \text{in} \ \mathcal{A}. \end{aligned} \tag{13}$$

https://doi.org/10.1017/S0263574721000333 Published online by Cambridge University Press

Now, it is seen from (13) that for given bounded Lévy characteristics $(\boldsymbol{\theta}_0, \boldsymbol{\Theta}_1, \varpi_j, j = 1, \cdots, m_2)$, minimizing $J(\boldsymbol{\tau}_e)$ will result in minimization of (a time-integration of) the magnitudes of the tracking errors $\boldsymbol{X}_e$ and the control $\boldsymbol{\tau}_e$. Moreover, the class $\mathcal{K}_\infty$-functions $\hat{\gamma}_i, i = 0, 1, 2$ and $\hat{\gamma}_{3j}$, and positive definite functions $\varphi(\boldsymbol{X}_e, t)$ (recalling that this case is inside of the set $\mathcal{A}$) and $S(\boldsymbol{X}_e, t)$ are the design functions. Thus, when $J(\boldsymbol{\tau}_e)$ is minimized, the affect of the Lévy characteristics on the robot is reduced, that is, disturbance attenuation is achieved.

(2) Outside of the set $\mathcal{A}$: In this case, we have the bounds:

$$\begin{aligned}(\|\boldsymbol{X}_e\| \le \delta) \cup \left(\lim_{t\to\infty} \sup \mathbb{E}\left\{\int_{t_0}^{t}\left[\varphi\left(\boldsymbol{X}_e, r\right) + \hat{\gamma}_2\left(\left\|\boldsymbol{R}_2^{\frac{1}{2}}\left(\boldsymbol{X}_e, r\right)\boldsymbol{\tau}_e\right\|\right)\right] dr\right\}\right) \\ \le \sup_{\mathcal{D}}\left(\lim_{t\to\infty} \sup \mathbb{E}\left\{\int_{t_0}^{t}\left[\hat{\gamma}_0\left(\|\boldsymbol{\theta}_0\|\right) + \hat{\gamma}_1\left(\|\boldsymbol{\Theta}_1\boldsymbol{\Theta}_1^T\|\right) + \sum_{j=1}^{m_2}\hat{\gamma}_{3j}\left(\varpi_j\right)\right] dr\right\}\right)\end{aligned} \tag{14}$$

regardless whether $J(\boldsymbol{\tau}_e)$ is minimized or not. The above inequality shows the disturbance attenuation because the class $\mathcal{K}_\infty$-functions $\hat{\gamma}_i, i = 0, 1, 2$ and $\hat{\gamma}_{3j}$, and positive definite function $\varphi(\boldsymbol{X}_e, t)$ are the design functions as discussed in the previous case. Since the tracking errors $\boldsymbol{X}_e$ and the control $\boldsymbol{\tau}_e$ have relatively small magnitudes in this case, their minimization is not critical.

3. Inverse optimal stabilization of systems driven by Lévy processes

This section presents a concept of SDEs driven by Lévy processes, definitions of solution and stability, and a Lyapunov-type theorem on well-posedness (existence and uniqueness) and stability of SDEs. Then, a theorem is developed to design an inverse optimal stabilizer for nonlinear systems driven by Lévy processes. The results in this section will be applied to mobile robots in Section 4.

3.1. Well-posedness and stability of SDEs

The following notations are taken from refs. [49, 50]. Let $\boldsymbol{W}(t), t \ge t_0 \ge 0$ be an m_1-dimensional standard Brownian motion vector defined on a complete probability space $(\Omega, \mathcal{F}, \mathbb{P})$ equipped with a filtration $\mathcal{F}_{t\ge t_0}$ such that it is right continuous and $\mathcal{F}_{t_0}$ contains all $\mathbb{P}$-null sets. Let $\boldsymbol{N} = \text{col}(N_1, ..., N_j, ..., N_{m_2})$ be an m_2-dimensional Poisson random measure vector defined on $\mathbb{R}^+ \times (\mathbb{R}^{m_2} - \{0\})$ with an m_2-dimensional compensator vector $\widetilde{\boldsymbol{N}}$ and m_2-dimensional intensity measure vector $\boldsymbol{\nu} = \text{col}(\nu_1, ..., \nu_j, ..., \nu_{m_2})$. Each Poisson measure $N_j((t_0, t] \times \mathbb{A})$ on a Borel measurable subset $\mathbb{A}$ with $j = 1, ..., m_2$ can be represented by a point process $q(s)$ with the domain $\mathcal{D}_q$ as a countable subset of $\mathbb{R}^+$, which is a collection of non-negative real numbers, that is, $N_j((t_0, t], \mathbb{A}) = \sum_{s\in\mathcal{D}_q, t_0\le s\le t} 1_{\mathbb{A}}(q(s))$, where $1_{\mathbb{A}}$ denotes the indicator function of the subset $\mathbb{A}$. We assume that all N_j are independent of each other, $\boldsymbol{N}$ is independent of $\boldsymbol{W}, \widetilde{\boldsymbol{N}}(dt, d\boldsymbol{\xi}) := \boldsymbol{N}(dt, d\boldsymbol{\xi}) - dt\boldsymbol{\nu}(d\boldsymbol{\xi})$, and $\int_{\mathbb{R}-\{0\}}(|\xi_j|^2 \wedge 1)\nu_j(d\xi_j) < \infty$. We consider the nonlinear SDE driven by Lévy processes:

$$\begin{aligned}&d\boldsymbol{X}(t) = \boldsymbol{F}(\boldsymbol{X}(t), t)dt + \boldsymbol{G}(\boldsymbol{X}(t), t)d\boldsymbol{W}(t) + \sum_{j=1}^{m_2}\int_{|\xi_j|<\varepsilon_j} \boldsymbol{\Phi}^{(j)}\left(\boldsymbol{X}\left(t^-\right), t, \xi_j\right)\widetilde{N}_j\left(dt, d\xi_j\right), \\ &\boldsymbol{X}(t_0) = \boldsymbol{X}_0 \in \mathbb{R}^n,\end{aligned} \tag{15}$$

where $\boldsymbol{X}(t^-) = \lim_{s\uparrow t}\boldsymbol{X}(s)$; $\boldsymbol{F} : \mathbb{R}^n \times [t_0, \infty) \to \mathbb{R}^n$, $\boldsymbol{G} : \mathbb{R}^n \times [t_0, \infty) \to \mathbb{R}^{n\times m_1}$, $\boldsymbol{\Phi}^{(j)} : \mathbb{R}^n \times [t_0, \infty) \times \mathbb{R} \to \mathbb{R}^n$. The constant $\varepsilon_j \in (0, \infty)$ is the jth maximum allowable jump size. We assume that $\boldsymbol{F}(\boldsymbol{X}(t), t)$, $\boldsymbol{G}(\boldsymbol{X}(t), t)$, and $\boldsymbol{\Phi}^{(j)}(\boldsymbol{X}(t^-), t, \xi_j)$ satisfy the following local conditions to ensure local well-posedness of (15).

https://doi.org/10.1017/S0263574721000333 Published online by Cambridge University Press

Assumption 3.1.
C1. [Local Lipschitz] For any $\boldsymbol{X}, \boldsymbol{Y} \in \mathbb{R}^n$ with $\|\boldsymbol{X}\| \vee \|\boldsymbol{Y}\| \leq \epsilon_1$, where ϵ_1 is a positive constant, there exists a nonnegative constant L_1 such that for all $t \in [t_0, \infty)$:

$$\|\boldsymbol{F}(\boldsymbol{X}, t) - \boldsymbol{F}(\boldsymbol{Y}, t)\|^2 + \|\boldsymbol{G}(\boldsymbol{X}, t) - \boldsymbol{G}(\boldsymbol{Y}, t)\|^2 + \sum_{j=1}^{m_2} \int_{|\xi_j|<\varepsilon_j} \|\boldsymbol{\Phi}^{(j)}\left(\boldsymbol{X}, t, \xi_j\right) - \boldsymbol{\Phi}^{(j)}\left(\boldsymbol{Y}, t, \xi_j\right)\|^2 \nu_j\left(d\xi_j\right)$$
$$\leq L_1 \|\boldsymbol{X} - \boldsymbol{Y}\|^2, \tag{16}$$

where $\boldsymbol{\Phi}^{(j)}$ is the jth column of $\boldsymbol{\Phi}$, and $\varepsilon_j \in (0, \infty]$.
C2. [Locally linear growth] For any $\boldsymbol{X} \in \mathbb{R}^n$ with $\|\boldsymbol{X}\| \leq \epsilon_2$, where ϵ_2 is a positive constant, there exists a nonnegative constant L_2 such that for all $t \in [t_0, \infty)$:

$$\|\boldsymbol{F}(\boldsymbol{X}, t)\|^2 + \|\boldsymbol{G}(\boldsymbol{X}, t)\|^2 + \sum_{j=1}^{m_2} \int_{|\xi_j|<\varepsilon_j} \|\boldsymbol{\Phi}^{(j)}\left(\boldsymbol{X}, t, \xi_j\right)\|^2 \nu_j(d\xi_j) \leq L_2\left(1 + \|\boldsymbol{X}\|^2\right). \tag{17}$$

We give definitions of solution and stability of (15), which are taken/motivated from refs. [27] and [24].

Definition 3.1. The process $\boldsymbol{X}(t)$ is called a solution of (15) if it is $\mathbb{R}^n$-valued $\mathcal{F}_t$-adapted and càdlàg and satisfies

$$\boldsymbol{X}(t) = \boldsymbol{X}_0 + \int_{t_0}^{t} \boldsymbol{F}(\boldsymbol{X}(s), s)ds + \int_{t_0}^{t} \boldsymbol{G}(\boldsymbol{X}(s), s)d\boldsymbol{W}(s) + \int_{t_0}^{t} \sum_{j=1}^{m_2} \int_{|\xi_j|<\varepsilon_j} \boldsymbol{\Phi}^{(j)}\left(\boldsymbol{X}(s^-), s, \xi_j\right) \widetilde{N}_j\left(ds, d\xi_j\right). \tag{18}$$

Definition 3.2. Let α be a class $\mathcal{K}_\infty$-function, ϵ be a positive constant, and ϵ_0 be a nonnegative constant. The trivial solution of (15) is said to be

- globally practically $\mathcal{K}_\infty$-exponentially p-stable (or globally practically $\mathcal{K}_\infty$-exponentially stable in the p^{th} moment, where $p \geq 1$ is a positive constant) if
$$\mathbb{E}\{\|\boldsymbol{X}(t)\|^p\} \leq \alpha(\|\boldsymbol{X}(t_0)\|^p)e^{-\epsilon(t-t_0)} + \epsilon_0, \tag{19}$$
for all $\boldsymbol{X}_0 \in \mathbb{R}^n$ with $\|\boldsymbol{X}_0\|^p < \infty$, and $t \in [t_0, \infty)$,
- almost surely (a.s.) globally practically $\mathcal{K}_\infty$-exponentially stable if
$$\|\boldsymbol{X}(t)\| \leq \alpha(\|\boldsymbol{X}(t_0)\|)e^{-\epsilon(t-t_0)} + \epsilon_0, \ \ a.s. \tag{20}$$
for all $\boldsymbol{X}(t_0) \in \mathbb{R}^n$ with $\|\boldsymbol{X}(t_0)\| < \infty$, and $t \in [t_0, \infty)$.

If $\epsilon_0 = 0$, then "practically" is dropped from the above statements. Moreover, if $\alpha(\bullet) \equiv c\bullet$ with c being a positive constant, "$\mathcal{K}_\infty$" is dropped.

The following theorem gives sufficient conditions on global well-posedness and stability of the SDE (15).

Theorem 3.1. *Under Assumption 3.1, assume further that there exists a function* $U(\boldsymbol{X}, t) \in C^{2\times 1}(\mathbb{R}^n \times [t_0, \infty))$ *called a Lyapunov function, a constant* $p \geq 1$, *and class* $\mathcal{K}_\infty$*-functions* α_1 *and* α_2 *such that* $\forall$ $(\boldsymbol{X}, t) \in \mathbb{R}^n \times [t_0, \infty)$:

$$\alpha_1(\|\boldsymbol{X}\|^p) \leq U(\boldsymbol{X}, t) \leq \alpha_2(\|\boldsymbol{X}\|^p). \tag{21}$$

(1) [Well-posedness] Suppose that $\mathcal{L}U(\boldsymbol{X}, t)$ *satisfies*

$$\mathcal{L}U(\boldsymbol{X}, t) \leq c_3(1 + U(\boldsymbol{X}, t)) \tag{22}$$

https://doi.org/10.1017/S0263574721000333 Published online by Cambridge University Press

for all $(\boldsymbol{X}, t) \in \mathbb{R}^n \times [t_0, \infty)$*, where* c_3 *is a nonnegative constant. Then, the system (15) has a unique global solution for each* $\boldsymbol{X}_0 \in \mathbb{R}^n$.
(2) [Stability] Suppose that there exists a nonnegative function $\hat{c}_4(t)$*, which satisfies the PE condition*

$$\int_{t_0}^{t} \hat{c}_4(\tau) d\tau \geq c_4(t - t_0) \tag{23}$$

with c_4 *being a positive constant, and a nonnegative constant* c_0 *such that for all* $(\boldsymbol{X}, t) \in \mathbb{R}^n \times [t_0, \infty)$:

$$\mathcal{L}U(\boldsymbol{X}, t) \leq -\hat{c}_4(t) U(\boldsymbol{X}, t) + c_0. \tag{24}$$

Then, the trivial solution of the system (15) is both a.s. globally practically $\mathcal{K}_\infty$*-exponentially stable and globally practically* $\mathcal{K}_\infty$*-exponentially p-stable. Moreover,*

$$\|\boldsymbol{X}(t)\|^p \leq \alpha_1^{-1} \left[\alpha_2 \left(\|\boldsymbol{X}_0\|^p \right) e^{-\left(c_4 - \frac{c_0}{\lambda}\right)(t - t_0)} + \lambda \right], \ a.s. \tag{25}$$

and

$$\mathbb{E}\{\|\boldsymbol{X}(t)\|^p\} \leq \alpha_1^{-1} \left[\alpha_2 \left(\|\boldsymbol{X}_0\|^p \right) e^{-\left(c_4 - \frac{c_0}{\lambda}\right)(t - t_0)} + \lambda \right], \tag{26}$$

where the constant λ *is such that* $\lambda > \frac{c_0}{c_4}$.

If $c_0 = 0$*, then "practically" is dropped from the above statement. Moreover, if* $\alpha_1(\bullet) \equiv c_1 \bullet$ *and* $\alpha_2(\bullet) \equiv c_2 \bullet$*, where* c_1 *and* c_2 *are positive constants, "*$\mathcal{K}_\infty$*" is dropped.*

Proof. Proof of this theorem can be done by using the proof of Theorem 2.1 in ref. [39], and the following lemma. □

Lemma 3.1. *Suppose that* $x(t) \in \mathbb{R}^+$ *satisfies*

$$\dot{x} \leq -c(t)x + c_0, \quad x(t_0) \in \mathbb{R}^+, \tag{27}$$

where $c(t)$ *is a nonnegative function of* t *satisfies* $\int_{t_0}^{t} c(\tau) d\tau \geq c^*(t - t_0)$ *with* c^* *being a positive constant, and* c_0 *is a nonnegative constant. If* $c_0 = 0$*, then*

$$x(t) \leq x(t_0) e^{-c^*(t - t_0)}. \tag{28}$$

If $c_0 > 0$*, then*

$$x(t) \leq x(t_0) e^{-\left(c^* - \frac{c_0}{\lambda}\right)(t - t_0)} + \lambda, \tag{29}$$

where $\lambda > \frac{c_0}{c^*}$ *is a constant.*

Proof. If one directly solves the differential inequality (27) to obtain the bound for $x(t)$, it will be extremely hard because of the function $c(t)$. Here, a simple proof is provided. If $c_0 = 0$, then the comparison principle in ref. [24] and (27) implies that $x(t) \leq x(t_0) e^{-\int_{t_0}^{t} c(\tau) d\tau} \leq x(t_0) e^{-c^*(t - t_0)}$, which gives (28). Let us consider the case $c_0 > 0$. Define a ball $\mathcal{B}$ centered at the origin with a radius λ. It is sufficient to consider the case when $x(t_0) \notin \mathcal{B}$. Then, in this case, (27) implies that

$$\dot{x} \leq -c(t)x + \frac{c_0}{\lambda} x, \quad x(t) \notin \mathcal{B}. \tag{30}$$

By the comparison principle, we have

$$\begin{aligned} x(t) &\leq x(t_0) e^{-\int_{t_0}^{t} \left(c(\tau) - \frac{c_0}{\lambda}\right) d\tau} \\ &\leq x(t_0) e^{-\left(c^* - \frac{c_0}{\lambda}\right)(t - t_0)}, \end{aligned} \tag{31}$$

which yields (29) because $\lambda > \frac{c_0}{c^*}$ gives $c^* - \frac{c_0}{\lambda} > 0$ and $x(t_0) \notin \mathcal{B}$. □

https://doi.org/10.1017/S0263574721000333 Published online by Cambridge University Press

3.2. Inverse optimal stabilization design

Consider the following stochastic system driven by Lévy processes with unknown characteristics:

$$\begin{aligned} d\boldsymbol{X}(t) &= (\boldsymbol{F}(\boldsymbol{X}(t),t) + \boldsymbol{G}_0(\boldsymbol{X}(t),t)\boldsymbol{\theta}_0 + \boldsymbol{G}_2(\boldsymbol{X}(t),t)\boldsymbol{u})\,dt + \boldsymbol{G}_1(\boldsymbol{X}(t),t)\boldsymbol{\Theta}_1 d\boldsymbol{W}(t) \\ &\quad + \sum_{j=1}^{m_2} \boldsymbol{\Phi}^{(j)}\left(\boldsymbol{X}(t^-),t\right) \int_{|\xi_j|<\varepsilon_j} \widetilde{N}_j\left(dt, d\xi_j\right), \\ \boldsymbol{X}(t_0) &= \boldsymbol{X}_0 \in \mathbb{R}^n, \end{aligned} \tag{32}$$

where the drift vector $\boldsymbol{\theta}_0$ takes (unknown) values in $\mathbb{R}^{m_0}$, the covariance matrix $\boldsymbol{\Theta}_1$ of the Brownian motion vector $\boldsymbol{W}(t)$ takes values in the $m_1 \times m_1$ (unknown) nonnegative definite matrices, the integral of intensity measure $\varpi_j := \int_{|\xi_j|<\varepsilon_j} \nu_j(d\xi_j)$ takes (unknown) nonnegative values, $\boldsymbol{G}_0 : \mathbb{R}^n \times [t_0, \infty) \to \mathbb{R}^{n\times m_0}$, and all other symbols are defined in Subsection 3.1. We assume that $\boldsymbol{\theta}_0 \in \mathcal{D}_0$, $\boldsymbol{\Theta}_1 \in \mathcal{D}_1$, and $\boldsymbol{\varpi} \in \mathcal{D}_2$ with $\boldsymbol{\varpi} = \text{col}(\varpi_1, \cdots, \varpi_{m_2})$, where $\mathcal{D}_0$ is the set of locally bounded function of $(\boldsymbol{X}, t)$, while $\mathcal{D}_1$ and $\mathcal{D}_2$ are sets of locally bounded functions of $(\boldsymbol{X}, t)$ taking nonnegative values. The inverse optimal control design with gain assignment is stated in the following theorem.

Theorem 3.2. *Let $U(\boldsymbol{X}, t) \in C^{2\times 1}(\mathbb{R}^n \times [t_0, \infty))$ be a Lyapunov function candidate satisfying (21), γ_2 be a class $\mathcal{K}_\infty$-function γ_2 whose derivative γ_2' (defined as $\gamma_2'(r) = \frac{d\gamma_2(r)}{dr}$) is also a class $\mathcal{K}_\infty$-function, $\boldsymbol{R}_2(\boldsymbol{X}, t)$ be a symmetric positive definite matrix-valued function. Suppose that the control law ("inverse pre-optimal control")*

$$\boldsymbol{u} = \boldsymbol{\alpha}(\boldsymbol{X}, t) = -\boldsymbol{R}_2^{-1}\left(U_{\boldsymbol{X}}\boldsymbol{G}_2\right)^T \frac{\ell\gamma_2\left(\left\|U_{\boldsymbol{X}}\boldsymbol{G}_2\boldsymbol{R}_2^{-\frac{1}{2}}\right\|\right)}{\left\|U_{\boldsymbol{X}}\boldsymbol{G}_2\boldsymbol{R}_2^{-\frac{1}{2}}\right\|^2}, \tag{33}$$

where $\ell\gamma_2$ denotes the Legendre–Fenchel (LF) transform of γ_2, see Lemma A.2, is used for the auxiliary system of the system (32):

$$\begin{aligned} d\boldsymbol{X}(t) &= (\boldsymbol{F}(\boldsymbol{X}(t),t) + \boldsymbol{G}_0(\boldsymbol{X}(t),t)\bar{\boldsymbol{\theta}}_0 + \boldsymbol{G}_2(\boldsymbol{X}(t),t)\boldsymbol{u})dt + \boldsymbol{G}_1(\boldsymbol{X}(t),t)\overline{\boldsymbol{\Theta}}_1 d\boldsymbol{W}(t) \\ &\quad + \sum_{j=1}^{m_2} \boldsymbol{\Phi}^{(j)}(\boldsymbol{X}(t^-),t) \int_{|\xi_j|<\varepsilon_j} \widetilde{\overline{N}}_j\left(dt, d\xi_j\right), \\ \boldsymbol{X}(t_0) &= \boldsymbol{X}_0 \in \mathbb{R}^n, \end{aligned} \tag{34}$$

where $\bar{\boldsymbol{\theta}}_0 \in \mathbb{R}^{m_0}$; $\overline{\boldsymbol{\Theta}}_1 \in \mathbb{R}^{m_1\times m_1}$ and the intensity measure $\bar{\nu}_j$ of the compensator $\widetilde{\overline{N}}_j(dt, d\xi_j)$ are nonnegative and satisfy

$$\begin{aligned} \bar{\boldsymbol{\theta}}_0 &= \left(U_{\boldsymbol{X}}\boldsymbol{G}_0\right)^T \frac{\ell\gamma_0(\|U_{\boldsymbol{X}}\boldsymbol{G}_0\|)}{\|U_{\boldsymbol{X}}\boldsymbol{G}_0\|^2}, \\ \overline{\boldsymbol{\Theta}}_1\overline{\boldsymbol{\Theta}}_1^T &= 2\boldsymbol{G}_1^T U_{\boldsymbol{X}\boldsymbol{X}}\boldsymbol{G}_1 \frac{\ell\gamma_1\left(\|\boldsymbol{G}_1^T U_{\boldsymbol{X}\boldsymbol{X}}\boldsymbol{G}_1\|\right)}{\|\boldsymbol{G}_1^T U_{\boldsymbol{X}\boldsymbol{X}}\boldsymbol{G}_1\|^2}, \\ \int_{|\xi_j|<\varepsilon_j} \bar{\nu}_j\left(d\xi_j\right) &= \left(U(\boldsymbol{X}+\boldsymbol{\Phi}^{(j)},t) - U - U_{\boldsymbol{X}}\boldsymbol{\Phi}^{(j)}\right) \frac{\ell\gamma_{3j}\left(|U(\boldsymbol{X}+\boldsymbol{\Phi}^{(j)},t) - U - U_{\boldsymbol{X}}\boldsymbol{\Phi}^{(j)}|\right)}{|U(\boldsymbol{X}+\boldsymbol{\Phi}^{(j)},t) - U - U_{\boldsymbol{X}}\boldsymbol{\Phi}^{(j)}|^2}, \end{aligned} \tag{35}$$

https://doi.org/10.1017/S0263574721000333 Published online by Cambridge University Press

with γ_0, γ_1, and γ_{3j}, and their derivatives γ_0', γ_1', and γ_{3j}' being class $\mathcal{K}_\infty$-functions, guarantees

$$\begin{aligned}\mathcal{L}U(\boldsymbol{X},t)|_{(33)} =& U_t + U_{\boldsymbol{X}}\boldsymbol{F} + U_{\boldsymbol{X}}\boldsymbol{G}_0\boldsymbol{\theta}_0 + \tfrac{1}{2}Tr\left(\overline{\boldsymbol{\Theta}}_1^T\boldsymbol{G}_1^T U_{\boldsymbol{XX}}\boldsymbol{G}_1\overline{\boldsymbol{\Theta}}_1\right) + U_{\boldsymbol{X}}\boldsymbol{G}_2\boldsymbol{\alpha}(\boldsymbol{X},t)\\ &+\sum_{j=1}^{m_2}\left[U\left(\boldsymbol{X}+\boldsymbol{\Phi}^{(j)},t\right) - U - U_{\boldsymbol{X}}\boldsymbol{\Phi}^{(j)}\right]\int_{|\xi_j|<\varepsilon_j}\bar{\nu}_j(d\xi_j)\\ &\leq -\hat{c}_4(t)U(\boldsymbol{X},t) + c_0\end{aligned} \tag{36}$$

for a nonnegative function $\hat{c}_4(t)$ satisfying $\int_{t_0}^{t}\hat{c}_4(\tau)d\tau \geq c_4(t-t_0)$ with c_4 being a positive constant, and a nonnegative constant c_0. Then,

$$\boldsymbol{u}^\star = \boldsymbol{\alpha}^\star(\boldsymbol{X},t) = -\frac{\beta}{2}\boldsymbol{R}_2^{-1}\left(U_{\boldsymbol{X}}\boldsymbol{G}_2\right)^T\frac{(\gamma_2')^{-1}\left(\left\|U_{\boldsymbol{X}}\boldsymbol{G}_2\boldsymbol{R}_2^{-\frac{1}{2}}\right\|\right)}{\left\|U_{\boldsymbol{X}}\boldsymbol{G}_2\boldsymbol{R}_2^{-\frac{1}{2}}\right\|}, \tag{37}$$

for all $\beta \geq 2$, is an a.s. and in the pth moment inverse optimal gain assignment control law for (32), which is continuous away from the origin and minimizes the cost function:

$$\begin{aligned}J(\boldsymbol{u}) = \sup_{\mathcal{D}}\Bigg(\lim_{t\to\infty}\sup\mathbb{E}\Bigg\{2\beta U\left(\boldsymbol{X}(t),t\right) + \int_{t_0}^{t}\Bigg[\varphi(\boldsymbol{X},\tau) + \beta^2\gamma_2\left(\frac{2}{\beta}\left\|\boldsymbol{R}_2^{\frac{1}{2}}\boldsymbol{u}\right\|\right) - \beta\lambda_0\gamma_0\left(\frac{2\|\boldsymbol{\theta}_0\|}{\lambda_0}\right)\\ -\beta\lambda_1\gamma_1\left(\frac{\|\boldsymbol{\Theta}_1\boldsymbol{\Theta}_1^T\|}{\lambda_1}\right) - 2\beta\sum_{j=1}^{m_2}\mu_j\gamma_{3j}\left(\frac{1}{\mu_j}\varpi_j\right)\Bigg]d\tau\Bigg\}\Bigg),\end{aligned} \tag{38}$$

where $\mathcal{D} := (\boldsymbol{\theta}_0, \boldsymbol{\Theta}_1, \boldsymbol{\varpi}) \in \mathcal{D}_0 \times \mathcal{D}_1 \times \mathcal{D}_2$, $0 < \lambda_0 \leq 2$, $0 < \lambda_1 \leq 2$, $0 < \mu_j \leq 1$, and

$$\begin{aligned}\varphi(\boldsymbol{X},t) = 2\beta[&\ell\gamma_2\left(\left\|U_{\boldsymbol{X}}\boldsymbol{G}_2\boldsymbol{R}_2^{-\frac{1}{2}}\right\|\right) - U_t - U_{\boldsymbol{X}}\boldsymbol{F} - \ell\gamma_0\left(\|U_{\boldsymbol{X}}\boldsymbol{G}_0\|\right) - \ell\gamma_1\left(\|\boldsymbol{G}_1^T U_{\boldsymbol{XX}}\boldsymbol{G}_1\|\right)\\ &-\sum_{j=1}^{m_2}\ell\gamma_{3j}\left(\left|U\left(\boldsymbol{X}+\boldsymbol{\Phi}^{(j)},t\right) - U - U_{\boldsymbol{X}}\boldsymbol{\Phi}^{(j)}\right|\right] + \beta(\beta-2)\ell\gamma_2\left(\left\|U_{\boldsymbol{X}}\boldsymbol{G}_2\boldsymbol{R}_2^{-\frac{1}{2}}\right\|\right)\\ &+\beta(2-\lambda_0)\ell\gamma_0\left(\|U_{\boldsymbol{X}}\boldsymbol{G}_0\|\right) + \beta(2-\lambda_1)\ell\gamma_1\left(\|\boldsymbol{G}_1^T U_{\boldsymbol{XX}}\boldsymbol{G}_1\|\right)\\ &+2\beta\sum_{j=1}^{m_2}\left(1-\mu_j\right)\ell\gamma_{3j}\left(\left|U\left(\boldsymbol{X}+\boldsymbol{\Phi}^{(j)},t\right) - U - U_{\boldsymbol{X}}\boldsymbol{\Phi}^{(j)}\right|\right).\end{aligned} \tag{39}$$

Moreover, the Lyapunov function candidate $U(\boldsymbol{X},t)$ solves the following family of HJI equations parameterized by $\beta \in [2,\infty)$, $\lambda_0 \in (0,2]$, $\lambda_1 \in (0,2]$, and $\mu_j \in (0,1]$:

$$\begin{aligned}U_t + U_{\boldsymbol{X}}\boldsymbol{F} + \frac{\lambda_0}{2}\ell\gamma_0\left(\|U_{\boldsymbol{X}}\boldsymbol{G}_0\|\right) + \frac{\lambda_1}{2}\ell\gamma_1\left(\|\boldsymbol{G}_1^T U_{\boldsymbol{XX}}\boldsymbol{G}_1\|\right) + \sum_{j=1}^{m_2}\mu_j\ell\gamma_{3j}\left(\left|U\left(\boldsymbol{X}+\boldsymbol{\Phi}^{(j)},t\right) - U - U_{\boldsymbol{X}}\boldsymbol{\Phi}^{(j)}\right|\right)\\ -\frac{\beta}{2}\ell\gamma_2\left(\left|U_{\boldsymbol{X}}\boldsymbol{G}_2\boldsymbol{R}_2^{-\frac{1}{2}}\right|\right) + \frac{\varphi(\boldsymbol{X},t)}{2\beta} = 0.\end{aligned} \tag{40}$$

Proof. Since this theorem is more general than the ones in refs. [26, 43, 51] in the sense that it considers the drift component of the Lévy processes, $\hat{c}_4(t)$ in (36) is allowed to be a nonnegative function of t instead of a positive constant, and the constant c_0 appears in (36), a proof is given in Appendix B. □

https://doi.org/10.1017/S0263574721000333 Published online by Cambridge University Press

Remark 3.1.

(1) The inverse optimal control $\boldsymbol{u}^{\star}$ has an infinite gain margin because $\beta \geq 2$. This is an important property for robustness, see ref. [40]. As seen from Theorem 3.2 that it is not required to a HJI to design an inverse optimal gain assignment control law. However, the Lyapunov function $U(\boldsymbol{X}, t)$ is a solution to the HJI Eq. (40). Moreover, the cost function $J(\boldsymbol{u})$ given by (38) is resulted after the control design instead of being pre-specified. It is seen from the cost function $J(\boldsymbol{u})$ that the disturbance attenuation can be achieved arbitrarily by choosing appropriate class $\mathcal{K}_{\infty}$-functions γ_0, γ_1, and γ_{3j}, see also Remark 2.2. As shown in Appendix B that the function $\varphi(\boldsymbol{X}, t)$ is positive definite for all $\|\boldsymbol{X}\|^p > \alpha_1^{-1}(c_0/c_4)$ and $t \in [t_0, \infty)$, the cost function $J(\boldsymbol{u})$ is meaningful because it is positive definite in both the state $\boldsymbol{X}$ (whenever $\|\boldsymbol{X}\|^p > \alpha_1^{-1}(c_0/c_4)$) and the control $\boldsymbol{u}$ since γ_2 is a class $\mathcal{K}_{\infty}$-function.

(2) In recent direct optimal control designs proposed in refs. [52, 53, 54], with an assumption on known Lévy process characteristics $(\boldsymbol{\Theta}_0, \boldsymbol{\Theta}_1, \boldsymbol{\varpi})$ (otherwise the HJB Eq. (13) in ref. [54] is not solvable for example) and on structure of $\boldsymbol{G}_1\boldsymbol{\Theta}_1, \boldsymbol{G}_2, \boldsymbol{R}_2$, a HJB equation used in the optimal control design can be transformed (via a logarithmic transformation) into a simpler partial differential equation (PDE). However, a numerical scheme is still required to solve this PDE (whereas Theorem 3.2 does not require to solve any HJB equation because U is a solution to the HJB Eq. (40)).

4. Inverse optimal control design for mobile robots

The control design consists of three steps by applying the backstepping method in ref. [25]. In the first step, the linear velocity $\frac{r}{2}(\omega_1 + \omega_2)$ and heading angle ϕ are viewed as immediate controls to stabilize the position tracking errors $(x - x_d, y - y_d)$. In the second step, the angular velocity $\frac{r}{2b}(\omega_1 - \omega_2)$ is viewed as an immediate control to stabilize the error between the virtual heading angle and its actual value. In the last step, the actual control torque vector $\boldsymbol{\tau}$ will be designed to stabilize the errors between the virtual linear and angular velocities and their actual values. Convergence of the heading angle to its reference value will be ensured through the above control design steps. Differently from the existing works in control of mobile robots reviewed in Section 1, the above steps will be carried out such that Control Objective 2.1 is fulfilled, that is, exponential stability of the tracking errors in the pth moment and a.s., and a meaningful cost function is minimized. In the control design, we choose quartic Lyapunov function candidates instead of a quadratic one due to the diffusion term $\boldsymbol{\Theta}_1(t)d\boldsymbol{W}(t)$ in the Lévy processes.

4.1. Step 1

Define

$$\begin{aligned} &x_e = x - x_d, \;\; y_e = y - y_d, \\ &\phi_e = \phi - \alpha_{\phi}, \;\; \omega_{ie} = \omega_i - \alpha_{\omega_i}, \;\; i = 1, 2, \end{aligned} \tag{41}$$

where α_{ϕ} and α_{ω_i} are referred to as virtual controls of ϕ and ω_i, respectively. Differentiating the first two equations of (41) along the solutions of the first two equations of (5) gives

$$\begin{aligned} dx_e &= \left[\frac{r}{2}\left(\alpha_{\omega_1} + \alpha_{\omega_2}\right)\cos\left(\alpha_{\phi}\right) - \bar{u}_d\cos(\phi_d)\,\dot{s}\right]dt + (\Delta_{11} + \Delta_{12})\,dt, \\ dy_e &= \left[\frac{r}{2}\left(\alpha_{\omega_1} + \alpha_{\omega_2}\right)\sin\left(\alpha_{\phi}\right) - \bar{u}_d\sin(\phi_d)\,\dot{s}\right]dt + (\Delta_{21} + \Delta_{22})\,dt, \end{aligned} \tag{42}$$

where

$$\begin{aligned} \Delta_{11} &= \frac{r}{2}\left(\alpha_{\omega_1} + \alpha_{\omega_2}\right)\left(\cos(\phi) - \cos\left(\alpha_{\phi}\right)\right), \quad \Delta_{12} = \frac{r}{2}\left(\omega_{1e} + \omega_{2e}\right)\cos(\phi), \\ \Delta_{21} &= \frac{r}{2}\left(\alpha_{\omega_1} + \alpha_{\omega_2}\right)\left(\sin(\phi) - \sin\left(\alpha_{\phi}\right)\right), \quad \Delta_{22} = \frac{r}{2}\left(\omega_{1e} + \omega_{2e}\right)\sin(\phi). \end{aligned} \tag{43}$$

https://doi.org/10.1017/S0263574721000333 Published online by Cambridge University Press

To design the virtual controls $\frac{r}{2}(\alpha_{\omega_1}+\alpha_{\omega_2})$ and α_ϕ that stabilize (x_e, y_e), we consider the Lyapunov function candidate

$$U_1 = \frac{1}{4}\left(x_e^4 + y_e^4\right). \tag{44}$$

Applying the Itô formula, see Lemma A.1, to U_1 along the solutions of (42) yields

$$\begin{aligned}\mathcal{L}U_1 = x_e^3\left[\frac{r}{2}\left(\alpha_{\omega_1}+\alpha_{\omega_2}\right)\cos\left(\alpha_\phi\right) - \bar{u}_d\cos(\phi_d)\,\dot{s}\right] + y_e^3\left[\frac{r}{2}\left(\alpha_{\omega_1}+\alpha_{\omega_2}\right)\sin\left(\alpha_\phi\right) - \bar{u}_d\sin(\phi_d)\,\dot{s}\right]\\ + x_e^3\left(\Delta_{11}+\Delta_{12}\right) + y_e^3\left(\Delta_{21}+\Delta_{22}\right).\end{aligned} \tag{45}$$

To ensure that exponential stability of (x_e, y_e), we design

$$\begin{aligned}\frac{r}{2}\left(\alpha_{\omega_1}+\alpha_{\omega_2}\right)\cos\left(\alpha_\phi\right) - \bar{u}_d\cos(\phi_d)\,\dot{s} &= f_{x_e},\\ \frac{r}{2}\left(\alpha_{\omega_1}+\alpha_{\omega_2}\right)\sin\left(\alpha_\phi\right) - \bar{u}_d\sin(\phi_d)\,\dot{s} &= f_{y_e},\\ \dot{s} &= kk_0(t)\sqrt{1+x_e^2+y_e^2},\end{aligned} \tag{46}$$

where

$$f_{x_e} = -k_1k_0^2(t)\bar{u}_d^2x_e, \quad f_{y_e} = -k_2k_0^2(t)\bar{u}_d^2y_e. \tag{47}$$

k_1 and k_2 are positive constants to be chosen later; k and $k_0(t)$ are a constant and a time-varying function, respectively, that will be chosen for the desired rate $\dot{s}_d$ of the reference path parameter s. This can be seen from the expression of $\dot{s}$ in (46) that when (x_e, y_e) converge to zero (or to neighborhood of the origin), which is guaranteed by the subsequent control design, $\dot{s}$ converges to its desired value $\dot{s}_d = kk_0(t)$. Thus, specifying k and $k_0(t)$ yields the desired rate $\dot{s}_d$ of the path-parameter s. It will be seen shortly that the design of $\dot{s}$ in (46) is to ensure that $\frac{r}{2}(\alpha_{\omega_1}+\alpha_{\omega_2})$ and α_ϕ are solvable for all $(x_e, y_e)\in\mathbb{R}^2$ provided that the control gains k, k_1, k_2 are appropriately chosen. This will yield global exponential stability of the closed-loop system later. Solving the first two equations of (46) yields

$$\begin{aligned}\alpha_\phi &= \phi_d + \arctan\left(\frac{A_{11}}{A_{12}}\right),\\ \frac{r}{2}\left(\alpha_{\omega_1}+\alpha_{\omega_2}\right) &= \left(\bar{u}_d\cos(\phi_d)\,\dot{s}+f_{x_e}\right)\cos\left(\alpha_\phi\right) + \left(\bar{u}_d\sin(\phi_d)\,\dot{s}+f_{y_e}\right)\sin\left(\alpha_\phi\right)\\ \Rightarrow \alpha_{\omega_1}+\alpha_{\omega_2} &= \frac{2}{r}\left(\left(\bar{u}_d\cos(\phi_d)\,\dot{s}+f_{x_e}\right)\cos\left(\alpha_\phi\right) + \left(\bar{u}_d\sin(\phi_d)\,\dot{s}+f_{y_e}\right)\sin\left(\alpha_\phi\right)\right) := A_{21},\end{aligned} \tag{48}$$

where

$$\begin{aligned}A_{11} &= k_1k_0(t)\bar{u}_d\sin(\phi_d)x_e - k_2k_0(t)\bar{u}_d\cos(\phi_d)y_e,\\ A_{12} &= k\sqrt{1+x_e^2+y_e^2} - k_1k_0(t)\bar{u}_d\cos(\phi_d)x_e - k_2k_0(t)\bar{u}_d\sin(\phi_d)y_e.\end{aligned} \tag{49}$$

To ensure that α_ϕ is well defined for all $(x_e, y_e)\in\mathbb{R}^2$, under given $k, k_0(t), \bar{u}_d$ we choose k_1, k_2 such that

$$(k_1+k_2)|k_0(t)\bar{u}_d| < k, \tag{50}$$

for all $t\in\mathbb{R}^+$ and $s\in\mathbb{R}$. Then, α_ϕ and $\frac{r}{2}(\alpha_{\omega_1}+\alpha_{\omega_2})$ are smooth functions of $(x_e, y_e, \phi_d, \bar{u}_d, k_0(t))$. Substituting (46) into (42) results in

$$\begin{aligned}dx_e &= \left(f_{x_e}+\Delta_{11}+\Delta_{12}\right)dt := \bar{f}_{x_e}dt,\\ dy_e &= \left(f_{y_e}+\Delta_{21}+\Delta_{22}\right)dt := \bar{f}_{y_e}dt.\end{aligned} \tag{51}$$

https://doi.org/10.1017/S0263574721000333 Published online by Cambridge University Press

Substituting (46) into (45) gives

$$\mathcal{L}U_1 = -k_1 k_0^2(t)\bar{u}_d^2 x_e^4 - k_2 k_0^2(t)\bar{u}_d^2 y_e^4 + x_e^3(\Delta_{11} + \Delta_{12}) + y_e^3(\Delta_{21} + \Delta_{22}). \tag{52}$$

4.2. Step 2

In this step, we view $\frac{r}{2b}(\omega_1 - \omega_2)$ as an immediate control to stabilize ϕ_e. Differentiating the third equation in (41) along the solutions of the third equation in (5) with α_ϕ being given by (48) yields

$$d\phi_e = \left[\frac{r}{2b}\left(\alpha_{\omega_1} - \alpha_{\omega_2}\right) + \frac{r}{2b}\left(\omega_{1e} - \omega_{2e}\right) + f_{\phi_e} - \frac{\partial \alpha_\phi}{\partial x_e}\Delta_{12} - \frac{\partial \alpha_\phi}{\partial y_e}\Delta_{22}\right] dt, \tag{53}$$

with

$$f_{\phi_e} = -\frac{\partial \alpha_\phi}{\partial x_e}\left(f_{x_e} + \Delta_{11}\right) - \frac{\partial \alpha_\phi}{\partial y_e}\left(f_{y_e} + \Delta_{21}\right) - \frac{\partial \alpha_\phi}{\partial \phi_d}\dot{\phi}_d - \frac{\partial \alpha_\phi}{\partial \bar{u}_d}\dot{\bar{u}}_d - \frac{\partial \alpha_\phi}{\partial k_0(t)}\dot{k}_0(t). \tag{54}$$

where $\dot{\phi}_d = \frac{\partial \phi_d}{\partial s}\dot{s}$ and $\dot{\bar{u}}_d = \frac{\partial \bar{u}_d}{\partial s}\dot{s}$ with $\dot{s}$ being given by (46). To design the virtual control $\frac{r}{2b}(\alpha_{\omega_1} - \alpha_{\omega_2})$ that stabilizes ϕ_e, we consider the Lyapunov function candidate

$$U_2 = U_1 + \frac{1}{4}\phi_e^4. \tag{55}$$

Applying the Itô formula to U_2 along the solutions of (52) and (53) yields

$$\begin{aligned}\mathcal{L}U_2 = &-k_1 k_0^2(t)\bar{u}_d^2 x_e^4 - k_2 k_0^2(t)\bar{u}_d^2 y_e^4 + \phi_e^3\left[\frac{r}{2b}(\alpha_{\omega_1} - \alpha_{\omega_2}) + \frac{r}{2b}(\omega_{1e} - \omega_{2e}) + f_{\phi_e}\right] + x_e^3\Delta_{11} + y_e^3\Delta_{21}\\ &+ \left(x_e^3 - \frac{\partial \alpha_\phi}{\partial x_e}\phi_e^3\right)\Delta_{12} + \left(y_e^3 - \frac{\partial \alpha_\phi}{\partial y_e}\phi_e^3\right)\Delta_{22}.\end{aligned} \tag{56}$$

From (56), we choose

$$\begin{aligned}&\frac{r}{2b}(\alpha_{\omega_1} - \alpha_{\omega_2}) = -\left(k_3 + k_{31}x_e^4 + k_{32}y_e^4\right)\phi_e - f_{\phi_e}\\ &\Rightarrow \alpha_{\omega_1} - \alpha_{\omega_2} = -\frac{2b}{r}\left(\left(k_3 + k_{31}x_e^4 + k_{32}y_e^4\right)\phi_e + f_{\phi_e}\right) := A_{22},\end{aligned} \tag{57}$$

where k_3, k_{31}, and k_{32} are positive constants. Inclusion of $-(k_{31}x_e^4 + k_{32}y_e^4)\phi_e$ is to handle the terms $x_e^3\Delta_{11}$ and $y_e^3\Delta_{21}$ because these terms cannot be canceled in the next steps due to the use of quartic Lyapunov function candidates, which are required for handling the diffusion term $\boldsymbol{\Theta}_1(t)d\boldsymbol{W}(t)$. Substituting (57) into (56) gives

$$\begin{aligned}\mathcal{L}U_2 = &-k_1 k_0^2(t)\bar{u}_d^2 x_e^4 - k_2 k_0^2(t)\bar{u}_d^2 y_e^4 - \left(k_3 + k_{31}x_e^4 + k_{32}y_e^4\right)\phi_e^4 + \frac{r}{2b}\left(\omega_{1e} - \omega_{2e}\right)\phi_e^3 + x_e^3\Delta_{11} + y_e^3\Delta_{21}\\ &+ \left(x_e^3 - \frac{\partial \alpha_\phi}{\partial x_e}\phi_e^3\right)\Delta_{12} + \left(y_e^3 - \frac{\partial \alpha_\phi}{\partial y_e}\phi_e^3\right)\Delta_{22}.\end{aligned} \tag{58}$$

Substituting (57) into (53) yields

$$d\phi_e = \left[-\left(k_3 + k_{31}x_e^4 + k_{32}y_e^4\right)\phi_e + \frac{r}{2b}\left(\omega_{1e} - \omega_{2e}\right) - \frac{\partial \alpha_\phi}{\partial x_e}\Delta_{12} - \frac{\partial \alpha_\phi}{\partial y_e}\Delta_{22}\right] dt := \bar{f}_{\phi_e} dt. \tag{59}$$

Solving the second equation in (48) and (57) for α_{ω_1} and α_{ω_2} gives

$$\alpha_{\omega_1} = \frac{A_{21} + A_{22}}{2}, \quad \alpha_{\omega_2} = \frac{A_{21} - A_{22}}{2}. \tag{60}$$

https://doi.org/10.1017/S0263574721000333 Published online by Cambridge University Press

4.3. Step 3

This is the last step. We will apply Theorem 3.2. Define

$$\boldsymbol{\omega}_e = \begin{bmatrix} \omega_{1e} \\ \omega_{2e} \end{bmatrix}, \quad \boldsymbol{\alpha}_{\boldsymbol{\omega}} = \begin{bmatrix} \alpha_{\omega_1} \\ \alpha_{\omega_2} \end{bmatrix}. \tag{61}$$

Since α_{ω_1} and α_{ω_2} are smooth functions of $(x_e, y_e, \phi_e, \phi_d, \phi_d', \bar{u}_d, \bar{u}_d', k_0(t), \dot{k}_0(t))$, where $\phi_d' = \frac{\partial \phi_d}{\partial s}$ and $\bar{u}_d' = \frac{\partial \bar{u}_d}{\partial s}$, differentiating the first equation in (61) along the solutions of (51), (59), and the last equation in (5) yields

$$\boldsymbol{M} d\boldsymbol{\omega}_e = \left[-\boldsymbol{C}(\omega_1 - \omega_2)\boldsymbol{\omega} - \boldsymbol{D}\boldsymbol{\omega} + \boldsymbol{\tau} + \boldsymbol{F}_3 + \boldsymbol{\theta}_0(t)\right] dt + \boldsymbol{\Theta}_1(t) d\boldsymbol{W}(t) + \sum_{j=1}^{m_2} \boldsymbol{\Phi}^{(j)}(t) \int_{|\xi_j|<\varepsilon_j} d\widetilde{N}_j\left(dt, d\xi_j\right), \tag{62}$$

where

$$\boldsymbol{F}_3 = -\boldsymbol{M}\left(\frac{\partial \boldsymbol{\alpha}_{\boldsymbol{\omega}}}{\partial x_e}\bar{f}_{x_e} + \frac{\partial \boldsymbol{\alpha}_{\boldsymbol{\omega}}}{\partial y_e}\bar{f}_{y_e} + \frac{\partial \boldsymbol{\alpha}_{\boldsymbol{\omega}}}{\partial \phi_e}\bar{f}_{\phi_e} + \frac{\partial \boldsymbol{\alpha}_{\boldsymbol{\omega}}}{\partial \phi_d}\dot{\phi}_d + \frac{\partial \boldsymbol{\alpha}_{\boldsymbol{\omega}}}{\partial \phi_d'}\dot{\phi}_d' + \frac{\partial \boldsymbol{\alpha}_{\boldsymbol{\omega}}}{\partial \bar{u}_d}\dot{\bar{u}}_d + \frac{\partial \boldsymbol{\alpha}_{\boldsymbol{\omega}}}{\partial \bar{u}_d'}\dot{\bar{u}}_d'\right). \tag{63}$$

To stabilize $\boldsymbol{\omega}_e$, we choose the Lyapunov function candidate

$$U_3 = U_2 + \frac{1}{4}\left(\boldsymbol{\omega}_e^T \boldsymbol{M} \boldsymbol{\omega}_e\right)^2. \tag{64}$$

According to Theorem 3.2, the auxiliary system for (62) is

$$\boldsymbol{M} d\boldsymbol{\omega}_e = \left[-\boldsymbol{C}(\omega_1 - \omega_2)\boldsymbol{\omega} - \boldsymbol{D}\boldsymbol{\omega} + \boldsymbol{\tau} + \boldsymbol{F}_3 + \bar{\boldsymbol{\theta}}_0\right] dt + \overline{\boldsymbol{\Theta}}_1 d\boldsymbol{W}(t) + \sum_{j=1}^{m_2} \boldsymbol{\Phi}^{(j)}(t) \int_{|\xi_j|<\varepsilon_j} d\widetilde{\bar{N}}_j\left(dt, d\xi_j\right), \tag{65}$$

where

$$\begin{aligned} \bar{\boldsymbol{\theta}}_0 &= U_{3\boldsymbol{\omega}_e}^T \frac{\ell \gamma_0(\|U_{3\boldsymbol{\omega}_e}\|)}{\|U_{3\boldsymbol{\omega}_e}\|^2}, \\ \overline{\boldsymbol{\Theta}}_1 \overline{\boldsymbol{\Theta}}_1^T &= 2U_{3\boldsymbol{\omega}_e\boldsymbol{\omega}_e} \frac{\ell \gamma_1(\|U_{3\boldsymbol{\omega}_e\boldsymbol{\omega}_e}\|)}{\|U_{3\boldsymbol{\omega}_e\boldsymbol{\omega}_e}\|^2}, \\ \int_{|\xi_j|<\varepsilon_j} \bar{\nu}_j(d\xi_j) &= \left(U_3(\boldsymbol{\omega}_e + \boldsymbol{\Phi}^{(j)}) - U_3 - U_{3\boldsymbol{\omega}_e}\boldsymbol{\Phi}^{(j)}\right) \frac{\ell \gamma_{3j}\left(|U_3(\boldsymbol{\omega}_e + \boldsymbol{\Phi}^{(j)}) - U_3 - U_{3\boldsymbol{\omega}_e}\boldsymbol{\Phi}^{(j)}|\right)}{|U_3\left(\boldsymbol{\omega}_e + \boldsymbol{\Phi}^{(j)}\right) - U_3 - U_{3\boldsymbol{\omega}_e}\boldsymbol{\Phi}^{(j)}|^2}, \end{aligned} \tag{66}$$

with $\gamma_i, i = 0, 1, 3j$ being class $\mathcal{K}_\infty$-functions, whose derivatives $\gamma_i', i = 0, 1, 3j$ are also class $\mathcal{K}_\infty$-functions. For simplicity, we choose

$$\gamma_i(r) = \frac{1}{2}r^2, \tag{67}$$

which results in $\ell\gamma_i(r) = \frac{1}{2}r^2$. Applying the Itô formula to U_3 along the solutions of (58) and (65), and using the expressions of Δ_{12} and Δ_{22} given by (43) yields

$$\begin{aligned} \mathcal{L}U_3 = &-k_1 k_0^2(t)\bar{u}_d^2 x_e^4 - k_2 k_0^2(t)\bar{u}_d^2 y_e^4 - \left(k_3 + k_{31}x_e^4 + k_{32}y_e^4\right)\phi_e^4 + \frac{r}{2b}(\omega_{1e} - \omega_{2e})\phi_e^3 + x_e^3\Delta_{11} + y_e^3\Delta_{21} \\ &+ \left(x_e^3 - \frac{\partial \alpha_\phi}{\partial x_e}\phi_e^3\right)\Delta_{12} + \left(y_e^3 - \frac{\partial \alpha_\phi}{\partial y_e}\phi_e^3\right)\Delta_{22} + (\boldsymbol{\omega}_e^T \boldsymbol{M} \boldsymbol{\omega}_e)\boldsymbol{\omega}_e^T\left[-\boldsymbol{D}\boldsymbol{\omega}_e + \boldsymbol{F} + \boldsymbol{\tau} - \boldsymbol{\tau}_d\right] \\ &+ \ell\gamma_0\left(\|U_{3\boldsymbol{\omega}_e}\|\right) + \ell\gamma_1\left(\|U_{3\boldsymbol{\omega}_e\boldsymbol{\omega}_e}\|\right) + \sum_{j=1}^{m_2} \ell\gamma_{3j}\left(|U_3(\boldsymbol{\omega}_e + \boldsymbol{\Phi}^{(j)}) - U_3 - U_{3\boldsymbol{\omega}_e}\boldsymbol{\Phi}^{(j)}|\right) \end{aligned} \tag{68}$$

https://doi.org/10.1017/S0263574721000333 Published online by Cambridge University Press

where we have used the fact that $\boldsymbol{\omega_e}^T\boldsymbol{C}(\omega_1-\omega_2)\boldsymbol{\omega_e}=0$ because $\boldsymbol{C}$ is skew-symmetric, see (2), and

$$\boldsymbol{F}=\boldsymbol{C}(\omega_{1d}-\omega_{2d})\boldsymbol{\omega}_d+\boldsymbol{D}\boldsymbol{\omega}_d+\boldsymbol{M}\dot{\boldsymbol{\omega}}_d-\boldsymbol{C}(\omega_1-\omega_2)\alpha_{\boldsymbol{\omega}}-\boldsymbol{D}\boldsymbol{\alpha}_{\boldsymbol{\omega}}+\boldsymbol{F}_3. \tag{69}$$

The reference velocity vector is given by $\boldsymbol{\omega}_d=[\omega_{1d}\ \omega_{2d}]^T$ with $\omega_{1d}=\frac{1}{r}kk_0(t)(\bar{u}_d+b\phi_d')$ and $\omega_{2d}=\frac{1}{r}kk_0(t)(\bar{u}_d-b\phi_d')$, which are obtained from (60), and $\dot{\boldsymbol{\omega}}_d=[\dot{\omega}_{1d}\ \dot{\omega}_{2d}]^T$ with $\dot{\omega}_{1d}=\frac{1}{r}k\dot{k}_0(t)(\bar{u}_d+b\phi_d')+\frac{1}{r}kk_0(t)(\bar{u}_d'+b\phi_d'')kk_0(t)$ and $\dot{\omega}_{2d}=\frac{1}{r}k\dot{k}_0(t)(\bar{u}_d-b\phi_d')+\frac{1}{r}kk_0(t)(\bar{u}_d'-b\phi_d'')kk_0(t)$. From (68), we design the following control law, which will be shown to be an inverse pre-optimal control according to Theorem 3.2, as follows:

$$\begin{aligned}\boldsymbol{\tau}&=\boldsymbol{\tau}_e+\boldsymbol{\tau}_d,\\ \boldsymbol{\tau}_e&=-\left(\boldsymbol{K}_4+k_5\|\boldsymbol{F}\|^{\frac{4}{3}}\boldsymbol{I}\right)\boldsymbol{\omega}_e,\end{aligned} \tag{70}$$

where $\boldsymbol{\tau}_d$ is given by (10), $\boldsymbol{K}_4$ is a positive definite matrix, k_5 is a positive constant, and $\boldsymbol{I}$ is a 2×2 identity matrix. Substituting (70) into (68)

$$\begin{aligned}\mathcal{L}U_3=&-k_1k_0^2(t)\bar{u}_d^2x_e^4-k_2k_0^2(t)\bar{u}_d^2y_e^4-(k_3+k_{31}x_e^4+k_{32}y_e^4)\phi_e^4+\frac{r}{2b}(\omega_{1e}-\omega_{2e})\,\phi_e^3+x_e^3\Delta_{11}+y_e^3\Delta_{21}\\&+\left(x_e^3-\frac{\partial\alpha_\phi}{\partial x_e}\phi_e^3\right)\Delta_{12}+\left(y_e^3-\frac{\partial\alpha_\phi}{\partial y_e}\phi_e^3\right)\Delta_{22}+\left(\boldsymbol{\omega}_e^T\boldsymbol{M}\boldsymbol{\omega}_e\right)\boldsymbol{\omega_e}^T\left[-\left(\boldsymbol{D}+\boldsymbol{K}_4+k_5\|\boldsymbol{F}\|^{\frac{4}{3}}\boldsymbol{I}\right)\boldsymbol{\omega}_e+\boldsymbol{F}\right]\\&+\ell\gamma_0\left(\|U_{3\boldsymbol{\omega_e}}\|\right)+\ell\gamma_1\left(\|U_{3\boldsymbol{\omega_e}\boldsymbol{\omega_e}}\|\right)+\sum_{j=1}^{m_2}\ell\gamma_{3j}\left(|U_3\left(\boldsymbol{\omega_e}+\boldsymbol{\Phi}^{(j)}\right)-U_3-U_{3\boldsymbol{\omega_e}}\boldsymbol{\Phi}^{(j)}|\right).\end{aligned} \tag{71}$$

To calculate the upper bound of the right-hand side of (71), we use (43), (48), (67), and Young's inequality to calculate the following bounds:

$$\begin{aligned}x_e^3\Delta_{11}&\le a_{11}x_e^4+a_{12}\phi_e^4x_e^4+a_{13}\phi_e^4y_e^4+a_{14}\phi_e^4,\\ y_e^3\Delta_{21}&\le a_{21}y_e^4+a_{22}\phi_e^4x_e^4+a_{23}\phi_e^4y_e^4+a_{24}\phi_e^4,\\ x_e^3\Delta_{12}&\le a_{31}x_e^4+a_{32}\left(\omega_{1e}^4+\omega_{2e}^4\right),\\ y_e^3\Delta_{22}&\le a_{41}y_e^4+a_{42}\left(\omega_{1e}^4+\omega_{2e}^4\right),\\ -\frac{\partial\alpha_\phi}{\partial x_e}\phi_e^3\Delta_{12}&\le a_{51}\phi_e^4+a_{52}\left(\omega_{1e}^4+\omega_{2e}^4\right),\\ -\frac{\partial\alpha_\phi}{\partial y_e}\phi_e^3\Delta_{22}&\le a_{61}\phi_e^4+a_{62}\left(\omega_{1e}^4+\omega_{2e}^4\right),\\ \frac{r}{2b}(\omega_{1e}-\omega_{2e})\,\phi_e^3&\le a_{71}\phi_e^4+a_{72}\left(\omega_{1e}^4+\omega_{2e}^4\right),\\ \left(\boldsymbol{\omega}_e^T\boldsymbol{M}\boldsymbol{\omega}_e\right)\boldsymbol{\omega_e}^T\boldsymbol{F}&\le a_{81}\|\boldsymbol{\omega}_e\|^4\|\boldsymbol{F}\|^{\frac{4}{3}}+a_{82},\\ \ell\gamma_0\left(\|U_{3\boldsymbol{\omega_e}}\|\right)&\le a_{91}\|\boldsymbol{\omega}_e\|^4+\breve{\gamma}_0\left(\frac{1}{a_{91}}\right),\\ \ell\gamma_1\left(\|U_{3\boldsymbol{\omega_e}\boldsymbol{\omega_e}}\|\right)&\le a_{92}\|\boldsymbol{\omega}_e\|^4+\breve{\gamma}_1\left(\frac{1}{a_{92}}\right),\\ \sum_{j=1}^{m_2}\ell\gamma_{3j}\left(|U_3\left(\boldsymbol{\omega_e}+\boldsymbol{\Phi}^{(j)}\right)-U_3-U_{3\boldsymbol{\omega_e}}\boldsymbol{\Phi}^{(j)}|\right)&\le a_{93}\|\boldsymbol{\omega}_e\|^4+\breve{\gamma}_3\left(\frac{1}{a_{93}}\right),\end{aligned} \tag{72}$$

https://doi.org/10.1017/S0263574721000333 Published online by Cambridge University Press

where $\lambda_M(\boldsymbol{M})$ denotes the maximum eigenvalue of $\boldsymbol{M}$, a_{9i}, $i = 0, 1, 3$ are positive constants, $\breve{\gamma}_i$, $i = 0, 1, 3$ are class $\mathcal{K}_\infty$-functions, and

$$
\begin{aligned}
a_{11} &= 4|\bar{u}_d|\epsilon_{11} + 2\left(2|\bar{u}_d| + k_1 k_0^2(t)\,\bar{u}_d^2\right)\epsilon_{12} + 2\left(2|\bar{u}_d| + k_2 k_0^2(t)\,\bar{u}_d^2\right)\epsilon_{13},\\
a_{12} &= 2\left(2|\bar{u}_d| + k_1 k_0^2(t)\,\bar{u}_d^2\right)\epsilon_{12}^*,\\
a_{13} &= 2\left(2|\bar{u}_d| + k_2 k_0^2(t)\,\bar{u}_d^2\right)\epsilon_{13}^*,\\
a_{14} &= 4|\bar{u}_d|\epsilon_{11}^*,\\
a_{21} &= 4|\bar{u}_d|\epsilon_{21} + 2\left(2|\bar{u}_d| + k_1 k_0^2(t)\,\bar{u}_d^2\right)\epsilon_{22} + 2\left(2|\bar{u}_d| + k_2 k_0^2(t)\,\bar{u}_d^2\right)\epsilon_{23},\\
a_{22} &= 2\left(2|\bar{u}_d| + k_1 k_0^2(t)\,\bar{u}_d^2\right)\epsilon_{22}^*,\\
a_{23} &= 2\left(2|\bar{u}_d| + k_2 k_0^2(t)\,\bar{u}_d^2\right)\epsilon_{23}^*,\\
a_{24} &= 4|\bar{u}_d|\epsilon_{21}^*,\\
a_{31} &= \frac{r}{2}\epsilon_{31},\ \ a_{32} = 4r\epsilon_{31}^*,\ a_{41} = \frac{r}{2}\epsilon_{32},\ \ a_{42} = 4r\epsilon_{32}^*,\\
a_{51} &= \frac{r\left(k + 2k_1|k_0(t)\,\bar{u}_d|\right)\epsilon_{33}}{2\left(k - (k_1 + k_2)\,|k_0(t)\,\bar{u}_d|\right)},\ \ a_{52} = \frac{r\left(k + 2k_1|k_0(t)\,\bar{u}_d|\right)\epsilon_{33}^*}{2\left(k - (k_1 + k_2)\,|k_0(t)\,\bar{u}_d|\right)},\\
a_{61} &= \frac{r\left(k + 2k_2|k_0(t)\,\bar{u}_d|\right)\epsilon_{34}}{2\left(k - (k_1 + k_2)\,|k_0(t)\,\bar{u}_d|\right)},\ \ a_{62} = \frac{r\left(k + 2k_2|k_0(t)\,\bar{u}_d|\right)\epsilon_{34}^*}{2\left(k - (k_1 + k_2)\,|k_0(t)\,\bar{u}_d|\right)},\\
a_{71} &= \frac{r}{2b}\epsilon_{35},\ \ a_{72} = \frac{4r}{b}\epsilon_{35}^*,\\
a_{81} &= \lambda_M(\boldsymbol{M})\,\epsilon_{41},\ a_{82} = \lambda_M(\boldsymbol{M})\,\epsilon_{41}^*,
\end{aligned}
\tag{73}
$$

In (73), $\epsilon_{ij}, i = 1, \cdots, 4; j = 1, \cdots, 5$ are positive constants to be chosen, and $\epsilon_{ij}^* = \frac{27}{256\epsilon_{ij}^3}$. Substituting (72) into (71) yields

$$
\mathcal{L}U_3 \le -c_{11}x_e^4 - c_{12}y_e^4 - \left(c_{13} + c_{131}x_e^4 + c_{132}y_e^4\right)\phi_e^4 - c_{14}\|\boldsymbol{\omega}_e\|^4 - c_{141}\|\boldsymbol{\omega}_e\|^4\|\boldsymbol{F}\|^{\frac{4}{3}} + c_0, \tag{74}
$$

where

$$
\begin{aligned}
c_{11}(t) &= k_1 k_0^2(t)\bar{u}_d^2 - a_{11} - a_{31}\\
c_{12}(t) &= k_2 k_0^2(t)\bar{u}_d^2 - a_{21} - a_{41},\\
c_{13} &= k_3 - a_{14} - a_{24} - a_{51} - a_{61} - a_{71},\\
c_{131} &= k_{31} - a_{12} - a_{22},\\
c_{132} &= k_{32} - a_{13} - a_{23},\\
c_{14} &= \lambda_m(\boldsymbol{M})\lambda_m(\boldsymbol{K}_4 + \boldsymbol{D}) - a_{32} - a_{42} - a_{52} - a_{62} - a_{72} - a_{91} - a_{92} - a_{93},\\
c_{141} &= k_5\lambda_m(\boldsymbol{M}) - a_{81},\\
c_0 &= a_{82} + \breve{\gamma}_0\left(\frac{1}{a_{91}}\right) + \breve{\gamma}_1\left(\frac{1}{a_{92}}\right) + \breve{\gamma}_3\left(\frac{1}{a_{93}}\right),
\end{aligned}
\tag{75}
$$

and $\lambda_m(\bullet)$ denotes the minimum eigenvalue of $\bullet$. Note that c_0 can be made arbitrarily small by choosing appropriate constants ϵ_{41}, a_{91}, a_{92}, and a_{93}. We choose the control gains $k_1, k_2, k_3, k_{31}, k_{32}, \boldsymbol{K}_4, k_5$, and the constants ϵ_{ij}, a_{91}, a_{92}, a_{93} such that

$$
\begin{gathered}
\int_{t_0}^{t} c_{11}(\tau)d\tau - a_{11} - a_{31} \ge c_{11}^*, \quad \int_{t_0}^{t} c_{12}(\tau)d\tau - a_{21} - a_{41} \ge c_{12}^*,\\
c_{13} \ge c_{13}^*,\ \ c_{131} \ge 0,\ \ c_{132} \ge 0, c_{14} \ge c_{14}^*, c_{141} \ge 0,
\end{gathered}
\tag{76}
$$

https://doi.org/10.1017/S0263574721000333 Published online by Cambridge University Press

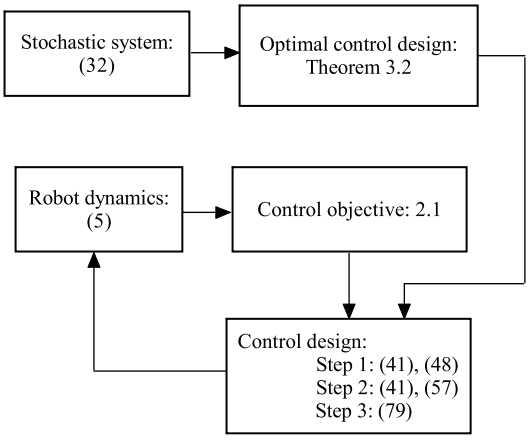


Figure 2. *Control design structure.*

where $c_{1i}^*, i = 1, \cdots, 4$ are strictly positive constants. Since $\dot{s}_d = kk_0(t)$ satisfies (7), there always exist the control gains $k_1, k_2, k_3, k_{31}, k_{32}, \boldsymbol{K}_4, k_5$, and the constants ϵ_{ij}, a_{91}, a_{92}, a_{93} such that the conditions in (76) hold. Under (76), we can write (74) as

$$\mathcal{L}U_3 \leq -c_3 U_3 + c_0, \tag{77}$$

where $c_3 = \frac{4\min(c_{11}^*, c_{12}^*, c_{13}^*, c_{14}^*)}{\max(1, \lambda_M^2(\boldsymbol{M}))}$.

The above inequality shows that the control law (70) both a.s. and in the pth moment globally practically exponentially stabilizes the auxiliary system consisting of (51), (59), and (65). To prove that the control law (70) is an inverse pre-optimal control according to Theorem 3.2, we need to show that it is of the form (33). In fact, choosing $\gamma_2(r) = \frac{1}{2}r^2$ gives $\ell\gamma_2(r) = \frac{1}{2}r^2$, see Lemma A.2. Then, it is seen that the control $\boldsymbol{\tau}_e$ given by (70) is of the form (33) with

$$\boldsymbol{R}_2 = \frac{1}{2}\boldsymbol{\omega}_e^T \boldsymbol{M}\boldsymbol{\omega}_e \boldsymbol{M}\left(\boldsymbol{K}_4 + k_4\|\boldsymbol{F}\|^{\frac{4}{3}}\boldsymbol{I}\right)^{-1}, \tag{78}$$

which is clearly positive definite. Hence, the control law given by (70) is an inverse pre-optimal control.

We now derive the inverse optimal control $\boldsymbol{\tau}_e^*$ based on the inverse pre-optimal control $\boldsymbol{\tau}_e$ given by (70). Since we chose $\gamma_2(r) = \frac{1}{2}r^2$, it yields that $(\gamma_2')^{-1}(r) = r$. Thus, the inverse optimal control is derived from (37) as

$$\begin{aligned} \boldsymbol{\tau}^\star &= \boldsymbol{\tau}_e^\star + \boldsymbol{\tau}_d, \\ \boldsymbol{\tau}_e^\star &= -\beta\left(\boldsymbol{K}_4 + k_5\|\boldsymbol{F}\|^{\frac{4}{3}}\boldsymbol{I}\right)\boldsymbol{\omega}_e, \end{aligned} \tag{79}$$

where $\beta \geq 2$ is a positive constant. The overall control design is summarized in Fig. 2

The inverse optimal control design for the mobile robots has been completed. We summarize the main results in the following theorem.

Theorem 4.1. *Under assumptions that the reference path satisfies the conditions (6) and (7), the inverse optimal control law $\boldsymbol{\tau}^\star$ given by (79) with $\boldsymbol{\tau}_d$ given by (10) solves Control Objective 2.1. In particular, this control law ensures global well-posedness and global practical exponential stability in the pth moment and a.s. of the closed-loop system consisting of (5) and (79). Moreover, the following cost function is minimized:*

https://doi.org/10.1017/S0263574721000333 Published online by Cambridge University Press



Figure 3. *The Khepera mobile robot.*

$$J(\boldsymbol{\tau}_e) = \sup_{\mathcal{D}} \left(\lim_{t\to\infty} \sup \mathbb{E} \left\{ 2\beta U_3(\boldsymbol{X}_e(t)) + \int_{t_0}^{t} [\varphi(\boldsymbol{X}_e) + \beta^2 \lambda_0 \gamma_2 \left(\frac{2}{\beta} \| \boldsymbol{R}_2^{\frac{1}{2}} \boldsymbol{\tau}_e \| \right) - \beta \lambda_0 \gamma_0 \left(\frac{2\|\boldsymbol{\theta}_0\|}{\lambda_0} \right) \right.$$
$$\left. - \beta \lambda_1 \gamma_1 \left(\frac{\|\boldsymbol{\Theta}_1 \boldsymbol{\Theta}_1^T\|}{\lambda_1} \right) - 2\beta \sum_{j=1}^{m_2} \mu_j \gamma_{3j} \left(\frac{1}{\mu_j} \varpi_j \right)] d\tau \right\} \right), \tag{80}$$

where $\boldsymbol{X}_e = [x_e \;\; y_e \;\; \phi_e \;\; \boldsymbol{\omega}_e^T]^T$, U_3 *is defined in (64),* $\boldsymbol{R}_2$ *is defined in (78),* $\gamma_i = \frac{1}{2} r^2$, $i = 0, 1, 2, 3j$,

$$\varphi(\boldsymbol{X}_e) = 2\beta \left[\ell\gamma_2 \left(\left\| U_{3\boldsymbol{X}_e} \boldsymbol{G}_2 \boldsymbol{R}_2^{-\frac{1}{2}} \right\| \right) - U_{3\boldsymbol{X}_e} \boldsymbol{F}_e - \ell\gamma_0 \left(\| U_{3\boldsymbol{X}_e} \boldsymbol{G}_0 \| \right) - \ell\gamma_1 \left(\boldsymbol{G}_1 \| U_{3\boldsymbol{X}_e \boldsymbol{X}_e} \boldsymbol{G}_1 \| \right) \right.$$
$$\left. - \sum_{j=1}^{m_2} \ell\gamma_{3j} \left(| U_3 \left(\boldsymbol{X}_e + \boldsymbol{\Phi}^{(j)} \right) - U_3 - U_{3\boldsymbol{X}_e} \boldsymbol{\Phi}^{(j)} | \right) \right] + \beta(\beta - 2) \ell\gamma_2 \left(\left\| U_{3\boldsymbol{X}_e} \boldsymbol{G}_2 \boldsymbol{R}_2^{-\frac{1}{2}} \right\| \right)$$
$$+ \beta(2 - \lambda_0) \ell\gamma_0 \left(\| U_{3\boldsymbol{X}_e} \boldsymbol{G}_0 \| \right) + \beta(2 - \lambda_1) \ell\gamma_1 \left(\left\| \boldsymbol{G}_1^T U_{3\boldsymbol{X}_e \boldsymbol{X}_e} \boldsymbol{G}_1 \right\| \right)$$
$$+ 2\beta \sum_{j=1}^{m_2} (1 - \mu_j) \ell\gamma_{3j} \left(| U_3 \left(\boldsymbol{X}_e + \boldsymbol{\Phi}^{(j)} \right) - U_3 - U_{3\boldsymbol{X}_e} \boldsymbol{\Phi}^{(j)} | \right), \tag{81}$$

and

$$\boldsymbol{G}_0 = \begin{bmatrix} \boldsymbol{0}_{3\times 2} \\ \boldsymbol{I} \end{bmatrix}, \boldsymbol{G}_1 = \begin{bmatrix} \boldsymbol{0}_{3\times 2} \\ \boldsymbol{I} \end{bmatrix}, \boldsymbol{G}_2 = \begin{bmatrix} \boldsymbol{0}_{3\times 2} \\ \boldsymbol{M} \end{bmatrix}. \tag{82}$$

Proof. Proof of this theorem directly follows Theorem 3.1. For a detailed elaboration of the cost function $J(\boldsymbol{\tau}_e)$ given by (80), see Remark 2.2. □

5. Experiments

This section presents experimental results on a small-size Khepera mobile robot (diameter of 0.07 m, height of 0.03 m, and weight of 0.08 kg), see Fig. 3, to verify the proposed controller designed in the previous section. Developed for educational and research purposes by K-Team (see the URL http://www.k-team.com for more information), the Khepera mobile robot consists of several proximity sensors (not used in the experiments) and can work in semi-autonomous (server–client) or completely autonomous mode. The Khepera mobile robot uses two DC motor-driven wheels. The DC motors are connected to the wheels through a 25:1 reduction gear box. Two incremental encoders are placed on the

https://doi.org/10.1017/S0263574721000333 Published online by Cambridge University Press

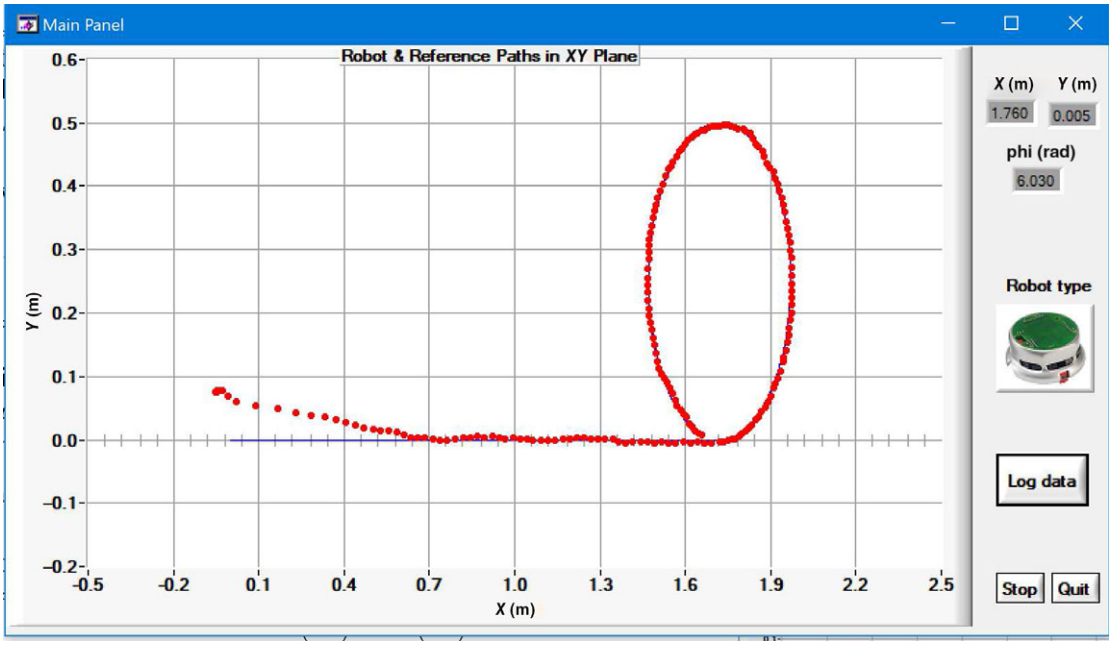


Figure 4. *Inverse optimal control: position in* (x, y) *plane.*

motor axes. The resolution of the encoder is 24 pulses per revolution of motor axis. This corresponds to $24 \times 25 = 600$ pulses per revolution of the wheels or 12 pulses per millimeter of wheel displacement. The algorithm to estimate the velocity from the encoder output is implemented on the robot. Communication between the Khepera mobile robot and a host computer is performed via a RS-232 serial port. We use the PCMCIA-232/4 card from National Instruments^{TM} for RS-232 communication between the robot and the host computer.

The physical parameters of the robot are: $b = 0.03$ m, $a = 0$ m, $r = 0.01$ m, $m_c = 0.07$ kg, $m_w = 0.005$ kg, $I_c = 0.04$ kgm^2, $I_w = 2.5 \times 10^{-5}$ kgm^2, $I_m = 1.25 \times 10^{-5}$ kgm^2, $d_{11} = d_{22} = 0.01$ kg/s. A program is written in LabWindows^{TM}/CVI (a C/C++ programming language with an easy development of user interface and hardware interface), a product of National Instruments^{TM}, to implement the control algorithm developed in this paper. In the experiment, the reference path is chosen as $x_d(s) = s$, $y_d(s) = 0$ for $t \leq 30$ s and $x_d(s) = x_d(s)|_{t=30} + 0.25 \sin(0.1s)$, $y_d(s) = y_d(s)|_{t=30} + 0.25(1 - cos(0.1s))$ for $t > 30$ s. This means that the reference path is a straight line followed by a circle. The desired rate of the path parameter is specified by $k = 2, k_0 = 1/2$. We generate the disturbances, which were modeled by Lévy processes in the previous section, by using a small gun bombarding sand onto the robot.

The control gains are chosen as $k_1 = 0.4, k_2 = 0.4, k_3 = 5, k_{31} = 1, k_{32} = 1, \boldsymbol{K}_4 = 10\boldsymbol{I}$, and $k_5 = 2$. It can be verified that all the conditions (50) and (76) hold.

We preform two experiments: inverse optimal control design, where the control $\boldsymbol{\tau}^\star$ is given by (79) with $\beta = 2$; inverse pre-optimal control design, where the control $\boldsymbol{\tau}$ is given by (70).

For the experimental results using the inverse optimal control design, Fig. 4 plots the robot and its reference paths in the (x, y)-plane; Fig. 5 plots the position tracking errors (x_e, y_e) in Fig. 5(a), heading error ϕ_e is plotted in Fig. 5(b), and the torques τ_1 and τ_2 are plotted in Fig. 5(c) (these are converted to control signals sent to the robot). The experimental results of the inverse pre-optimal control design are plotted in Figs. 6 and 7, whose explanations are the same as for the inverse optimal control design.

From these figures, it is seen that both control designs result in exponential convergence of the tracking errors and the noise (including random jumps) is due to the disturbances, which are due to sand bombarding on the robot. Moreover, the inverse optimal control design outperforms the inverse

https://doi.org/10.1017/S0263574721000333 Published online by Cambridge University Press

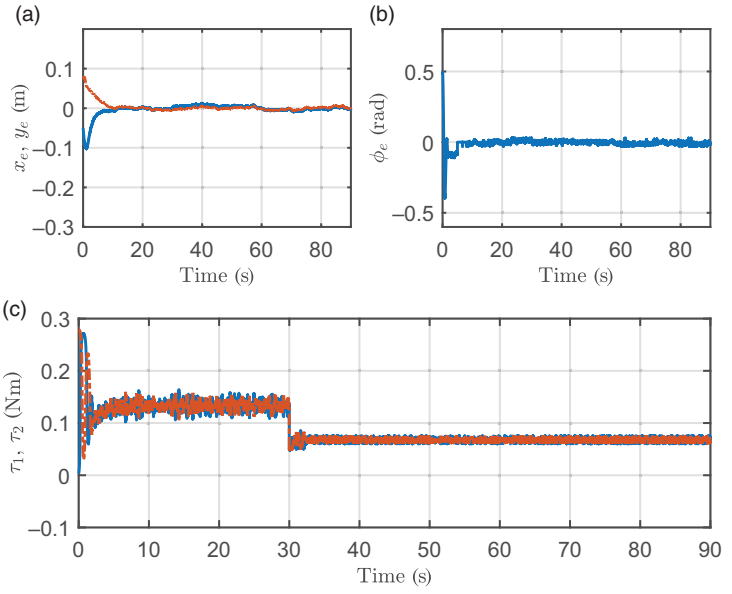


Figure 5. *Inverse optimal control: position errors, heading angle error, and control torques.*

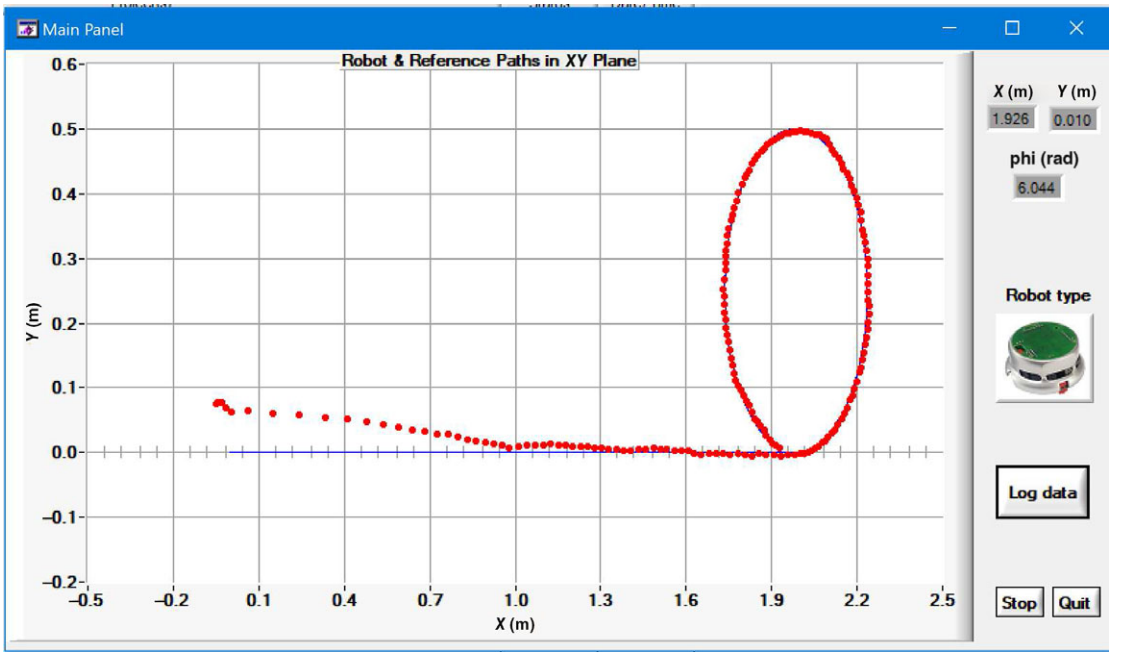


Figure 6. *Inverse pre-optimal control: position in* (x, y) *plane.*

pre-optimal control design. This is due to twofold. First, comparing Fig. 5(a) with Fig. 7(a) shows that the inverse optimal control yields much shorter transient response time of the position tracking errors (x_e, y_e) (about 10 s) than the inverse pre-optimal control (about 20 s). Moreover, comparing Fig. 5(b) with Fig. 7(b) shows that the inverse pre-optimal control yields more oscillation of the orientation error ϕ_e than the inverse optimal control. Second, from Fig. 8 in that the cost function $J(\boldsymbol{\tau}_e^{\star})$ resulted from the inverse optimal control design is much smaller (more than two times less) than the cost function

https://doi.org/10.1017/S0263574721000333 Published online by Cambridge University Press

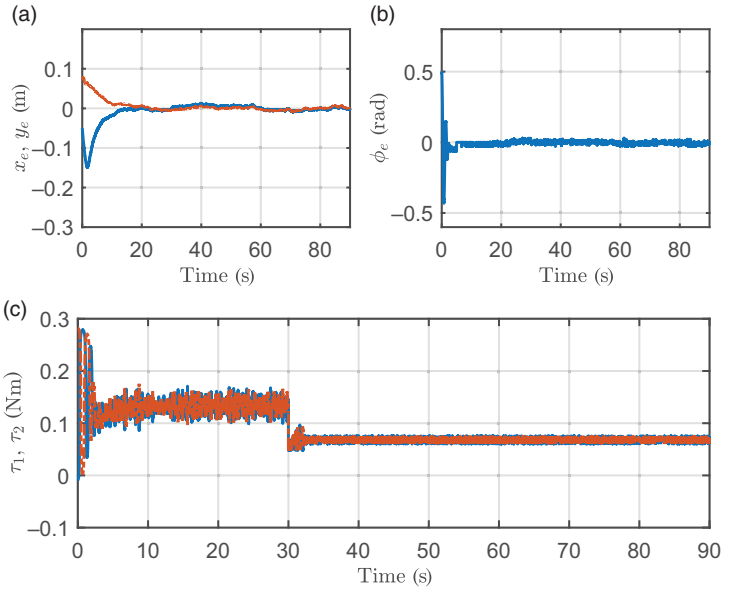


Figure 7. *Inverse pre-optimal control: position errors, heading angle error, and control torques.*

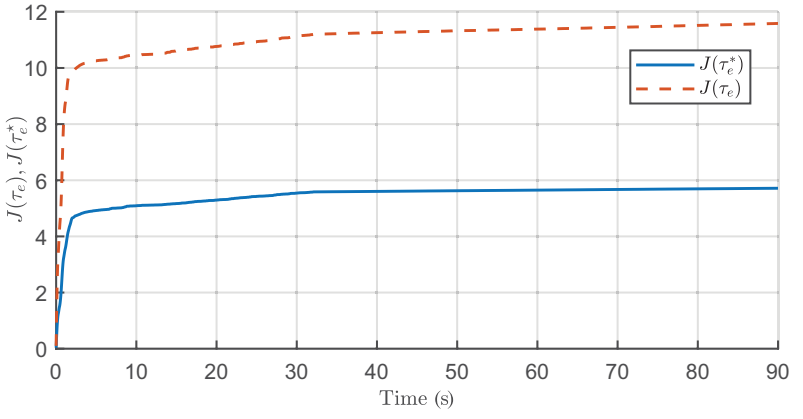


Figure 8. *Cost functions: $J(\boldsymbol{\tau}_e^\star)$ and $J(\boldsymbol{\tau}_e)$.*

$J(\boldsymbol{\tau}_e)$ resulted from the inverse pre-optimal control design. It is noted that other control designs in the existing literature (for example in refs. [9, 55]) will also result in poorer performance compared with either inverse optimal or inverse pre-optimal control design proposed in this paper in the sense that the existing control designs can only guarantee (practical) asymptotic convergence of the tracking errors when the reference path is a straight line, and only handle less general disturbances (no random jumps). More importantly, the existing control designs are not optimal as no cost function is minimized.

6. Conclusions

The new problem of inverse optimal path-tracking control design for mobile robots driven by Lévy processes has been formulated and solved in this paper. Two desired properties of the proposed control design include (1) global practical exponential stability both in the pth moment and a.s., where the reference path can be straight lines, curves, or their combination; and (2) minimization of a cost

https://doi.org/10.1017/S0263574721000333 Published online by Cambridge University Press

function that penalizes both path-tracking errors and the control torques without having to solve a HJI equation. The experimental results of both proposed inverse optimal and pre-optimal control laws on a small-size Khepera mobile robot showed practical exponential convergence of the tracking errors and out-performance of the inverse optimal control over the inverse pre-optimal control. The experiments effectively demonstrated theoretical developments summarized in Theorem 4.1. Future work is to apply the theoretical developments to design inverse optimal controllers for other underactuated mechanical systems.

References

[1] R. Murray and S. Sastry, "Nonholonomic motion planning: Steering using sinusoids", *IEEE Trans. Autom. Control* **38**(5), 700–716 (1993).

[2] I. Kolmanovsky and N. H. McClamroch, "Developments in nonholonomic control problems", *IEEE Control Syst. Mag.* **15**(6), 20–36 (1995).

[3] B. dAndrea Novel, G. Bastin and G. Campion, "Control of nonholonomic wheeled mobile robots by state feedback linearization", *Int. J. Rob. Res.* **14**(6), 543–559 (1995).

[4] A. M. Bloch and S. Drakunov, "Stabilization and tracking in the nonholonomic integrator via sliding mode", *Syst. Control Lett.* **29**(2), 91–99 (1996).

[5] R. W. Brockett, "Asymptotic Stability and Feedback Stabilization", **In:** *Differential Geometric Control Theory* (R. W. Brockett, R. S. Millman, and H. J. Sussmann, eds.) (Birkhauser, Boston, 1983) pp. 181–191.

[6] C. d. W. Canudas, B. Siciliano and G. Bastin, *Theory of Robot Control* (Springer, London, 1996).

[7] A. Astolfi, "Discontinuous control of the Brockett integrator", *Eur. J. Control* **4**(1), 49–63 (1998).

[8] T. C. Lee, K. T. Song, C. H. Lee and C. C. Teng, "Tracking control of unicycle-modelled mobile robots using a saturation feedback controller", *IEEE Trans. Control Syst. Technol.* **9**(2), 305–318 (2001).

[9] K. D. Do, Z. P. Jiang and J. Pan. "A global output-feedback controller for simultaneous tracking and stabilization of unicycle-type mobile robots", *IEEE Trans. Rob. Autom.* **20**(3), 589–594 (2004).

[10] K. D. Do, Z. P. Jiang and J. Pan. "Simultaneous stabilization and tracking control of mobile robots: An adaptive approach". *IEEE Trans. Autom. Control* **49**(7), 1147–1151 (2004).

[11] I. Zohar, A. Ailon and R. Rabinovici, "Mobile robot characterized by dynamic and kinematic equations and actuator dynamics: Trajectory tracking and related application," *Rob. Auton. Syst.* **59**(6), 343–353 (2011).

[12] S. Blazie, "A novel trajectory-tracking control law for wheeled mobile robots", *Rob. Auton. Syst.* **59**(11), 1001–1007 (2011).

[13] J. Huang, C. Wen, W. Wang and Z. P. Jiang, "Adaptive stabilization and tracking control of a nonholonomic mobile robot with input saturation and disturbance", *Syst. Control Lett.* **62**(3), 234–241 (2013).

[14] C. Samson, "Velocity and Torque Feedback Control of a Nonholonomic Cart", **In:** *Advanced Robot Control, Lecture Notes in Control and Information Sciences* (C. Canudas de Wit, ed.) (Berlin, Heidelberg, 1991) pp. 125–151.

[15] R. Fierro and F. L. Lewis, "Control of a Nonholonomic Mobile Robot: Backstepping Kinematics into Dynamics", *Proceedings of the 34th IEEE Conference on Decision and Control*, vol. 4, New Orleans, LA, USA (1995) pp. 3805–3810.

[16] K. D. Do, "Global output-feedback path-following control of unicycle-type mobile robots: A level curve approach", *Rob. Auton. Syst.* **74**(A), 229–242 (2015). doi: 10.1016/j.robot.2015.07.019.

[17] K. D. Do, "Bounded controllers for global path tracking control of unicycle-type mobile robots", *Rob. Auton. Syst.* **61**(8), 775–784 (2013).

[18] D. Soetanto, L. Lapierre and A. Pascoal, "Adaptive, Non-singular Path-Following Control of Dynamic Wheeled Robots". *Proceedings of the 42nd IEEE Conference on Decision and Control*, Maui (2003) pp. 1765–1770.

[19] K. D. Do and J. Pan, "Global output-feedback path tracking of unicycle-type mobile robots", *Rob. Comput. Integr. Manuf.* **22**(2), 166–179 (2006).

[20] K. D. Do and J. Pan, *Control of Ships and Underwater Vehicles* (Springer, London, 2009).

[21] M. Aicardi, G. Casalino, A. Bicchi and A. Balestrino, "Closed loop steering of unicycle-like vehicles via Lyapunov technique", *IEEE Rob. Autom. Mag.* **2**(1), 27–35 (1995).

[22] M. Egerstedt, X. Hu and A. Stotsky, "Control of mobile platforms using a virtual vehicle approach", *IEEE Trans. Autom. Control* **46**(11), 1777–1782 (2001).

[23] S. Sun and P. Cui, "Path tracking and a practical point stabilization of mobile robot", *Rob. Comput. Integr. Manuf.* **20**(1), 29–34 (2004).

[24] H. Khalil, *Nonlinear Systems* (Prentice Hall, New Jersey, 2002).

[25] M. Krstic, I. Kanellakopoulos and P. V. Kokotovic, *Nonlinear and Adaptive Control Design* (Wiley, New York, 1995).

[26] K. D. Do, "Inverse optimal gain assignment control of evolution systems and its application to boundary control of marine risers", *Automatica* **106**, 242–256 (2019). doi: 10.1016/j.automatica.2019.05.020.

[27] D. Applebaum, *Lévy Processes and Stochastic Calculus*, 2nd edn. (Cambridge University Press, New York, 2009).

[28] H. Deng, M. Krstic and R. Williams, "Stabilization of stochastic nonlinear systems driven by noise of unknown covariance", *IEEE Trans. Autom. Control* **46**(8), 1237–1253 (2001).

https://doi.org/10.1017/S0263574721000333 Published online by Cambridge University Press

[29] K. D. Do, "Global inverse optimal stabilization of stochastic nonholonomic systems", *Syst. Control Lett.* **75**, 41–55 (2015). doi: 10.1016/j.sysconle.2014.11.003.
[30] H. Deng and M. Krstic, "Stochastic nonlinear stabilization-part I: A backstepping design", *Syst. Control Lett.* **32**(3), 143–150 (1997).
[31] H. Wang and Q. Zhu, "Global stabilization of stochastic nonlinear systems via C^1 and C^∞ controllers", *IEEE Trans. Autom. Control* **62**(11), 5880–5887 (2017).
[32] H. Wang and Q. Zhu, "Finite-time stabilization of high-order stochastic nonlinear systems in strict-feedback form", *Automatica* **54**, 284–291 (2015). doi: 10.1016/j.automatica.2015.02.016.
[33] V. Barbu, F. Cordoni and L. Di Persio, "Optimal control of stochastic FitzHugh-Nagumo equation", *Int. J. Control* **89**(4), 746–756 (2016).
[34] J. Bennett and J. L. Wu, "An optimal control problem associated with SDEs driven by Lévy-type processes", *Stochastic Anal. Appl.* **26**, 471–494 (2008).
[35] H. Tang and Z. Wu, "Stochastic differential equations and stochastic linear quadratic optimal control problem with Lévy processes", *J. Syst. Sci. Complexity* **22**, 122–136 (2009). doi: 10.1007/s11424-009-9151-0.
[36] R. Singla, H. Parthasarathy, V. Agarwal and R. Rana, "Feedback optimization problem for master–slave teleoperation tracking in the presence of random noise in dynamics and feedback", *Nonlinear Dyn.* **86**, 559–586 (2016). doi: 10.1007/s11071-016-2908-9.
[37] P. Jagtap and M. Zamani, "Backstepping design for incremental stability of stochastic Hamiltonian systems with jumps", *IEEE Trans. Autom. Control* **63**(1), 255–261 (2018).
[38] K. D. Do and H. L. Nguyen, "Almost sure exponential stability of dynamical systems driven by Lévy processes and its application to control design for magnetic bearings", *Int. J. Control* (2018). doi: 10.1080/00207179.2018.1482502.
[39] K. D. Do, "Stochastic control of drill-heads driven by Lévy processes", *Automatica* **103**(2019), 36–45 (2019).
[40] R. Sepulchre, M. Jankovic and P. Kokotovic, *Constructive Nonlinear Control* (Springer, New York, 1997).
[41] M. Krstic and H. Deng, *Stabilization of Nonlinear Uncertain Systems* (Springer, London, 1998).
[42] H. Deng and M. Krstic, "Stochastic nonlinear stabilization-part II: inverse optimality", *Syst. Control Lett.* **32**(3), 151–159 (1997).
[43] K. D. Do, "Inverse optimal control of stochastic systems driven by Lévy processes", *Automatica* **107**, 539–550 (2019). doi: 10.1016/j.automatica.2019.06.016.
[44] T. Fukao, H. Nakagawa and N. Adachi, "Adaptive tracking control of a nonholonomic mobile robot", *IEEE Trans. Rob. Autom.* **16**(5), 609–615 (2000).
[45] W. Park, Y. Liu, Y. Zhou, M. Moses and G. S. Chirikjian, "Kinematic state estimation and motion planning for stochastic nonholonomic systems using the exponential map", *Robotica* **26**(4), 419–434 (2008).
[46] S. Thrun, W. Burgard and D. Fox, *Probabilistic Robotics* (The MIT Press, Cambridge, 2005).
[47] T. D. Barfoot and P. T. Furgale, "Associating uncertainty with three-dimensional poses for use in estimation problems", *IEEE Trans. Robot.* **30**(3), 679–693 (2014).
[48] H. T. Banks, J. L. Davis, S. L. Ernstberger, S. Hu, E. Artimovich, A. K. Dhar and C. L. Browdy, "A comparison of probabilistic and stochastic formulations in modelling growth uncertainty and variability", *J. Biol. Dyn.* **3**(2–3), 130–148 (2014).
[49] B. Øksendal and A. Sulem, *Applied Stochastic Control of Jump Diffusions*, 2nd edn. (Springer, Berlin, 2007).
[50] X. Mao, *Stochastic Differential Equations and Applications*, 2nd edn. (Woodhead publishing, Cambridge, 2007).
[51] K. D. Do, "Inverse optimal formation control of mobile agents with collision avoidance driven by Lévy processes", *IFAC J. Syst. Control* **13**, 100097:1–13 (2020). doi: 10.1016/j.ifacsc.2020.100097.
[52] Y. Pan, K. Bakshi and E. A. Theodorou, "Robust trajectory optimization: A cooperative stochastic game theoretic approach". *Rob. Sci. Syst.* (2015). doi: 10.15607/rss.2015.xi.029.
[53] K. Bakshi and E. A. Theodorou, "Infinite Dimensional Control of Doubly Stochastic Jump Diffusions", *Proceedings of the 55th IEEE Conference on Decision and Control*, Las Vegas (2016) pp. 1145–1152.
[54] E. A. Theodorou and E. Todorov, "Stochastic Optimal Control for Nonlinear Markov Jump Diffusion Processes", *Proceedings of 2012 American Control Conference*, Montréal, Canada (2012) pp. 1633–1639.
[55] K. D. Do and J. Pan, "Underactuated ships follow smooth paths with integral actions and without velocity measurements for feedback: Theory and experiments", *IEEE Trans. Control Syst. Technol.* **14**(2), 308–322 (2006).
[56] G. Hardy, J. E. Littlewood and G. Polya, *Inequalities*, 2nd edn. (Cambridge University Press, Cambridge, 1989).
[57] M. Krstic and Z. H. Li, "Inverse optimal design of input-to-state stabilizing nonlinear controllers". *IEEE Trans. Autom. Control* **43**(3), 336–350 (1998).

A. The Itô formula, LF transform, and general young's inequality

The Itô formula is given in the following lemma, see ref. [49].

Lemma A.1. *Let* $C^2(\mathbb{R}^n \times [t_0, \infty))$ *denote the space of all real-valued nonnegative functions* $U(\boldsymbol{X}, t)$ *on* $\mathbb{R}^n \times [t_0, \infty)$ *with the following properties:*

https://doi.org/10.1017/S0263574721000333 Published online by Cambridge University Press

- *$U(\boldsymbol{X},t)$ is twice (Fréchet) differentiable in $\boldsymbol{X}$ and is differentiable in t.*
- *All the $U_{\boldsymbol{X}}(\boldsymbol{X},t):=\frac{\partial U(\boldsymbol{X},t)}{\partial \boldsymbol{X}}$, $U_t(\boldsymbol{X},t):=\frac{\partial U(\boldsymbol{X},t)}{\partial t}$, and $U_{\boldsymbol{XX}}(\boldsymbol{X},t):=\frac{\partial^2 U(\boldsymbol{X},t)}{\partial \boldsymbol{X}^2}$ are continuous.*

Suppose that $\boldsymbol{X}(t), t\in[t_0,\infty)$, is a solution of (15). Then

$$\begin{aligned} U(\boldsymbol{X},t)=&U(\boldsymbol{X}_0,t_0)+\int_{t_0}^{t}\mathcal{L}U(\boldsymbol{X}(s),s)ds+\int_{t_0}^{t}U_{\boldsymbol{X}}(\boldsymbol{X}(s),s)\boldsymbol{G}(\boldsymbol{X}(s),s)d\boldsymbol{W}(s)\\ &+\int_{t_0}^{t}\sum_{j=1}^{m_2}\left[U\left(\boldsymbol{X}(s^-)+\boldsymbol{\Phi}^{(j)}\left(\boldsymbol{X}(s^-),s\right),s\right)-U\left(\boldsymbol{X}(s^-),s\right)\right]\int_{|\xi_j|<\varepsilon_j}\widetilde{N}_j\left(ds,d\xi_j\right), \end{aligned} \tag{A1}$$

where the infinite generator $\mathcal{L}U(\boldsymbol{X},t)$ is given by

$$\begin{aligned} \mathcal{L}U\left(\boldsymbol{X},t\right)=&U_t\left(\boldsymbol{X},t\right)+U_{\boldsymbol{X}}\left(\boldsymbol{X},t\right)\boldsymbol{F}\left(\boldsymbol{X},t\right)+\tfrac{1}{2}Tr\left(\boldsymbol{G}^T\left(\boldsymbol{X},t\right)U_{\boldsymbol{XX}}\left(\boldsymbol{X},t\right)\boldsymbol{G}\left(\boldsymbol{X},t\right)\right)\\ &+\sum_{j=1}^{m_2}[U\left(\boldsymbol{X}\left(t^-\right)+\boldsymbol{\Phi}^{(j)}\left(\boldsymbol{X}\left(t^-\right),t\right),t\right)-U\left(\boldsymbol{X}\left(t^-\right),t\right)-U_{\boldsymbol{X}}\left(\boldsymbol{X}\left(t^-\right),t\right)\boldsymbol{\Phi}^{(j)}\left(\boldsymbol{X}\left(t^-\right),t\right)]\varpi_j. \end{aligned} \tag{A2}$$

The operator Tr(•) denotes the trace of •, and it is recalled that $\varpi_j=\int_{|\xi_j|<\varepsilon_j}\nu_j(d\xi_j)$.
The LF transform is given in the following lemma.

Lemma A.2. *Let $\ell\gamma(r)$ denote the LF transform by (see ref. [56]:*

$$\ell\gamma(r)=r(\gamma')^{-1}(r)-\gamma((\gamma')^{-1}(r)), \tag{A3}$$

where $\gamma:\mathbb{R}\to\mathbb{R}$ is a class $\mathcal{K}_\infty$ function whose derivative $\gamma'(r)=\frac{d\gamma(r)}{dr}$ is also a class $\mathcal{K}_\infty$ function, and $(\gamma')^{-1}(r)$ denotes the inverse function of $\gamma'(r)$. The LF transform $\ell\gamma(r)$ has the following properties, see ref. [57]: (1) $\ell\gamma(r)=\int_0^r(\gamma')^{-1}(s)ds$; (2) $\ell\ell\gamma(r)=\gamma(r)$; (3) $\ell\gamma(r)$ is a class $\mathcal{K}_\infty$ function; (4) $\ell\gamma(\gamma'(r))=r\gamma'(r)-\gamma(r)$.

A.1. Young's inequality

For any $\boldsymbol{x},\boldsymbol{y}\in\mathbb{R}^n$, the Young inequality holds, see ref. [56]:

$$\boldsymbol{x}^T\boldsymbol{y}\le\gamma(\|\boldsymbol{x}\|)+\ell\gamma(\|\boldsymbol{y}\|), \tag{A4}$$

and the equality is achieved if and only if

$$\boldsymbol{y}=\gamma'(\|\boldsymbol{x}\|)\frac{\boldsymbol{x}}{\|\boldsymbol{x}\|}\Leftrightarrow\boldsymbol{x}=(\gamma')^{-1}(\|\boldsymbol{y}\|)\frac{\boldsymbol{y}}{\|\boldsymbol{y}\|}. \tag{A5}$$

B. Proof of Theorem 3.2

B.1. Proof of $J(\boldsymbol{u})$ being a meaningful cost functional

We first note from (35) that

$$\begin{aligned} &U_{\boldsymbol{X}}\boldsymbol{G}_0\bar{\boldsymbol{\theta}}_0=\ell\gamma_0\left(\|U_{\boldsymbol{X}}\boldsymbol{G}_0\|\right),\\ &\frac{1}{2}\mathrm{Tr}\left(\bar{\boldsymbol{\Theta}}_1^T\boldsymbol{G}_1^TU_{\boldsymbol{XX}}\boldsymbol{G}_1\bar{\boldsymbol{\Theta}}_1\right)=\ell\gamma_1\left(\|\boldsymbol{G}_1^TU_{\boldsymbol{XX}}\boldsymbol{G}_1\|\right),\\ &\left(U(\boldsymbol{X}+\boldsymbol{\Phi}^{(j)},t)-U-U_{\boldsymbol{X}}\boldsymbol{\Phi}^{(j)}\right)\int_{|\xi_j|<\varepsilon_j}\bar{\nu}_j(dt,d\xi_j=\ell\gamma_{3j}\left(|U(\boldsymbol{X}+\boldsymbol{\Phi}^{(j)},t)-U-U_{\boldsymbol{X}}\boldsymbol{\Phi}^{(j)}|\right). \end{aligned} \tag{B1}$$

Therefore, we can write (36) as

$$\begin{aligned} \mathcal{L}U(\boldsymbol{X},t)|_{(33)}=&U_t+U_{\boldsymbol{X}}\boldsymbol{F}+\ell\gamma_0\left(\|U_{\boldsymbol{X}}\boldsymbol{G}_0\|\right)+\ell\gamma_1\left(\|\boldsymbol{G}_1^TU_{\boldsymbol{XX}}\boldsymbol{G}_1\|\right)-\ell\gamma_2\left(\|U_{\boldsymbol{X}}\boldsymbol{G}_2\boldsymbol{R}_2^{-\frac{1}{2}}\|\right)\\ &+\sum_{j=1}^{m_2}\ell\gamma_{3j}\left(|U\left(\boldsymbol{X}+\boldsymbol{\Phi}^{(j)},t\right)-U-U_{\boldsymbol{X}}\boldsymbol{\Phi}^{(j)}|\right)\\ \le&-\hat{c}_4\left(t\right)U\left(\boldsymbol{X},t\right)+c_0. \end{aligned} \tag{B2}$$

https://doi.org/10.1017/S0263574721000333 Published online by Cambridge University Press

Substituting (B2) into (39) yields

$$\varphi(\boldsymbol{X},t)=\varphi_1(\boldsymbol{X},t)+\varphi_2(\boldsymbol{X},t), \tag{B3}$$

where

$$\begin{aligned}
&\varphi_1(\boldsymbol{X},t)=\beta\left(\hat{c}_4(t)\,U(\boldsymbol{X},t)-c_0\right),\\
&\varphi_2(\boldsymbol{X},t)=\beta(\beta-2)\,\ell\gamma_2\left(\|U_{\boldsymbol{X}}\boldsymbol{G}_2\boldsymbol{R}_2^{-\frac{1}{2}}\|\right)+\beta(2-\lambda_0)\,\ell\gamma_0\left(\|U_{\boldsymbol{X}}\boldsymbol{G}_0\|\right)+\beta(2-\lambda_1)\,\ell\gamma_1\left(\|\boldsymbol{G}_1^TU_{\boldsymbol{X}\boldsymbol{X}}\boldsymbol{G}_1\|\right)\\
&\qquad+2\beta\sum_{j=1}^{m_2}(1-\mu_j)\,\ell\gamma_{3j}\left(|U\left(\boldsymbol{X}+\boldsymbol{\Phi}^{(j)},t\right)-U-U_{\boldsymbol{X}}\boldsymbol{\Phi}^{(j)}|\right).
\end{aligned} \tag{B4}$$

Let us consider the integral:

$$\int_{t_0}^{t}\varphi_1(\boldsymbol{X}(\tau),\tau)d\tau=2\beta\int_{t_0}^{t}\left((\hat{c}_4(\tau)U(\boldsymbol{X}(\tau),\tau)-c_0)\right)d\tau. \tag{B5}$$

Define a ball $\mathcal{B}$ centered at the origin with a radius λ, where $\lambda>\frac{c_0}{c_4}$. Then, for $U(\boldsymbol{X},t)\notin\mathcal{B}$, it holds that

$$\int_{t_0}^{t}\varphi_1(\boldsymbol{X}(\tau),\tau)d\tau\geq 2\beta(c_4\lambda-c_0)(t-t_0) \tag{B6}$$

because $\int_{t_0}^{t}\hat{c}_4(\tau)d\tau\geq c_4(t-t_0)$, see (23). Therefore, $\int_{t_0}^{t}\varphi_1(\boldsymbol{X}(\tau),\tau)d\tau$ is positive as long as $U(\boldsymbol{X},t)>\frac{c_0}{c_4}$, that is, $\|\boldsymbol{X}\|^p>\alpha_1^{-1}(c_0/c_4)$ due to (21). Moreover, since $\beta\geq 2$, $0<\lambda_0\leq 2$, $0<\lambda_1\leq 2$, $0<\mu_j\leq 1$, $\ell\gamma_i, i=0,1,2$, and $\ell\gamma_{3j}$ are class $\mathcal{K}_\infty$ functions, $\varphi_2(\boldsymbol{X},t)$ is positive. Hence, $J(\boldsymbol{u})$ is meaningful.

B.2. Proof of $u^\star$ practically stabilizing (32)

The infinite generator $\mathcal{L}U$ along the control (37) is

$$\begin{aligned}
\mathcal{L}U|_{(37)}=&U_t+U_{\boldsymbol{X}}(\boldsymbol{F}+\boldsymbol{G}_0\boldsymbol{\theta}_0)+\frac{1}{2}\mathrm{Tr}\left(\boldsymbol{\Theta}_1^T\boldsymbol{G}_1^TU_{\boldsymbol{X}\boldsymbol{X}}\boldsymbol{G}_1\boldsymbol{\Theta}_1\right)-\frac{\beta}{2}U_{\boldsymbol{X}}\boldsymbol{G}_2\boldsymbol{R}_2^{-1}(U_{\boldsymbol{X}}\boldsymbol{G}_2)^T\frac{\left(\gamma_2'\right)^{-1}\left(\|U_{\boldsymbol{X}}\boldsymbol{G}_2\boldsymbol{R}_2^{-\frac{1}{2}}\|\right)}{\|U_{\boldsymbol{X}}\boldsymbol{G}_2\boldsymbol{R}_2^{-\frac{1}{2}}\|}\\
&+\sum_{j=1}^{m_2}[U\left(\boldsymbol{X}+\boldsymbol{\Phi}^{(j)},t\right)-U-U_{\boldsymbol{X}}\boldsymbol{\Phi}^{(j)}]\varpi_j.
\end{aligned} \tag{B7}$$

Using the general Young's inequality, we have

$$\begin{aligned}
&U_{\boldsymbol{X}}\boldsymbol{G}_0\boldsymbol{\theta}_0\leq\frac{\lambda_0}{2}\gamma_0\left(\frac{2\|\boldsymbol{\theta}_0\|}{\lambda_0}\right)+\frac{\lambda_0}{2}\ell\gamma_0\left(\|U_{\boldsymbol{X}}\boldsymbol{G}_0\|\right),\\
&\mathrm{Tr}\left(\boldsymbol{\Theta}_1^T\boldsymbol{G}_1^TU_{\boldsymbol{X}\boldsymbol{X}}\boldsymbol{G}_1\boldsymbol{\Theta}_1\right)\leq\lambda_1\gamma_1\left(\frac{\|\boldsymbol{\Theta}\boldsymbol{\Theta}^T\|}{\lambda_1}\right)+\lambda_1\ell\gamma_1\left(\|\boldsymbol{G}_1^TU_{\boldsymbol{X}\boldsymbol{X}}\boldsymbol{G}_1\|\right),\\
&\left[U\left(\boldsymbol{X}+\boldsymbol{\Phi}^{(j)},t\right)-U-U_{\boldsymbol{X}}\boldsymbol{\Phi}^{(j)}\right]\varpi_j\leq\mu_j\gamma_{3j}\left(\frac{\varpi_j}{\mu_j}\right)+\mu_j\ell\gamma_{3j}\left(|U\left(\boldsymbol{X}+\boldsymbol{\Phi}^{(j)},t\right)-U-U_{\boldsymbol{X}}\boldsymbol{\Phi}^{(j)}|\right).
\end{aligned} \tag{B8}$$

Substituting (B8) into (B7) and using (A3) yields

$$\begin{aligned}
\mathcal{L}U|_{(37)}\leq&U_t+U_{\boldsymbol{X}}\boldsymbol{F}+\frac{\lambda_0}{2}\ell\gamma_0\left(\|U_{\boldsymbol{X}}\boldsymbol{G}_0\|\right)+\frac{\lambda_1}{2}\ell\gamma_1\left(\|\boldsymbol{G}_1^TU_{\boldsymbol{X}\boldsymbol{X}}\boldsymbol{G}_1\|\right)+\frac{\lambda_0}{2}\gamma_0\left(\frac{2\|\boldsymbol{\theta}_0\|}{\lambda_0}\right)\\
&+\frac{\lambda_1}{2}\gamma_1\left(\frac{\|\boldsymbol{\Theta}_1\boldsymbol{\Theta}_1^T\|}{\lambda_1}\right)-\frac{\beta}{2}\ell\gamma_2\left(\|U_{\boldsymbol{X}}\boldsymbol{G}_2\boldsymbol{R}_2^{-\frac{1}{2}}\|\right)-\frac{\beta}{2}\gamma_2\left(\left(\gamma_2'\right)^{-1}\left(\|U_{\boldsymbol{X}}\boldsymbol{G}_2\boldsymbol{R}_2^{-\frac{1}{2}}\|\right)\right)+\sum_{j=1}^{m_2}\mu_j\gamma_{3j}\left(\frac{\varpi_j}{\mu_j}\right)\\
&+\sum_{j=1}^{m_2}\mu_j\ell\gamma_{3j}\left(|U\left(\boldsymbol{X}+\boldsymbol{\Phi}^{(j)},t\right)-U-U_{\boldsymbol{X}}\boldsymbol{\Phi}^{(j)}|\right).
\end{aligned} \tag{B9}$$

https://doi.org/10.1017/S0263574721000333 Published online by Cambridge University Press

Now substituting (35) into (36) yields

$$\begin{aligned}\mathcal{L}U(\boldsymbol{X},t)|_{(33)} &= U_t + U_{\boldsymbol{X}}\boldsymbol{F} + \ell\gamma_0\left(\|U_{\boldsymbol{X}}\boldsymbol{G}_0\|\right) + \ell\gamma_1\left(\|\boldsymbol{G}_1^T U_{\boldsymbol{XX}}\boldsymbol{G}_1\|\right) - \ell\gamma_2\left(\|U_{\boldsymbol{X}}\boldsymbol{G}_2\boldsymbol{R}_2^{-\frac{1}{2}}\|\right)\\ &\quad + \sum_{j=1}^{m_2}\ell\gamma_{3j}\left(|U\left(\boldsymbol{X}+\boldsymbol{\Phi}^{(j)},t\right) - U - U_{\boldsymbol{X}}\boldsymbol{\Phi}^{(j)}|\right)\\ &\le -\hat{c}_4(t)\,U(\boldsymbol{X},t) + c_0.\end{aligned} \tag{B10}$$

Substituting the last inequality in (B10) into (B9) gives

$$\begin{aligned}\mathcal{L}U|_{(37)} &\le -\hat{c}_4(t)U(\boldsymbol{X},t) - \frac{\beta}{2}\gamma_2\left(\left(\gamma_2'\right)^{-1}\left(\|U_{\boldsymbol{X}}\boldsymbol{G}_2\boldsymbol{R}_2^{-\frac{1}{2}}\|\right)\right)\\ &\quad + \frac{\lambda_0}{2}\gamma_0\left(\frac{2\|\boldsymbol{\theta}_0\|}{\lambda_0}\right) + \frac{\lambda_1}{2}\gamma_1\left(\frac{\|\boldsymbol{\Theta}_1\boldsymbol{\Theta}_1^T\|}{\lambda_1}\right) + \sum_{j=1}^{m_2}\mu_j\gamma_{3j}\left(\frac{\varpi_j}{\mu_j}\right) + c_0\end{aligned} \tag{B11}$$

because $\beta \ge 2$, $0 < \lambda_0 \le 2$, $0 < \lambda_1 \le 2$, and $0 < \mu_j \le 1$. By Theorem 3.1, the control (37) both a.s. globally practically $\mathcal{K}_\infty$-exponentially stabilizes the system (32) and globally practically $\mathcal{K}_\infty$-exponentially stabilizes the system (32) in the pth moment. Moreover, due to (B10), proof of well-posedness of the closed-loop system is followed from Theorem 3.1.

B.3. Proof of optimality

We first calculate $\mathcal{L}U$ along the solutions of (32) with the control (33), then use the general Young's inequality as:

$$\begin{aligned}\mathcal{L}U(\boldsymbol{X},t)|_{(33)} &= U_t + U_{\boldsymbol{X}}\boldsymbol{F} + U_{\boldsymbol{X}}\boldsymbol{G}_0\boldsymbol{\theta}_0 + U_{\boldsymbol{X}}\boldsymbol{G}_2\boldsymbol{\alpha}(\boldsymbol{X},t) + \tfrac{1}{2}\mathrm{Tr}\left(\boldsymbol{\Theta}_1^T\boldsymbol{G}_1^T U_{\boldsymbol{XX}}\boldsymbol{G}_1\boldsymbol{\Theta}_1\right)\\ &\quad + \sum_{j=1}^{m_2}[U\left(\boldsymbol{X}+\boldsymbol{\Phi}^{(j)},t\right) - U - U_{\boldsymbol{X}}\boldsymbol{\Phi}^{(j)}]\varpi_j\\ &\le U_t + U_{\boldsymbol{X}}\boldsymbol{F} + \gamma_0\left(\|\boldsymbol{\theta}_0\|\right) + \ell\gamma_0\left(\|U_{\boldsymbol{X}}\boldsymbol{G}_0\|\right) + \frac{1}{2}\gamma_1\left(\|\boldsymbol{\Theta}_1\boldsymbol{\Theta}_1^T\|\right) + \ell\gamma_1\left(\|\boldsymbol{G}_1^T U_{\boldsymbol{XX}}\boldsymbol{G}_1\|\right)\\ &\quad - \ell\gamma_2\left(\|U_{\boldsymbol{X}}\boldsymbol{G}_2\boldsymbol{R}_2^{-\frac{1}{2}}\|\right) + \sum_{j=1}^{m_2}\gamma_{3j}\left(\varpi_j\right)\sum_{j=1}^{m_2}\ell\gamma_{3j}\left(|U\left(\boldsymbol{X}+\boldsymbol{\Phi}^{(j)},t\right) - U - U_{\boldsymbol{X}}\boldsymbol{\Phi}^{(j)}|\right)\\ &\le -c_4U(\boldsymbol{X},t) + c_0 + \gamma_0\left(\|\boldsymbol{\theta}_0\|\right) + \frac{1}{2}\gamma_1\left(\|\boldsymbol{\Theta}\boldsymbol{\Theta}^T\|\right) + \sum_{j=1}^{m_2}\gamma_{3j}\left(\varpi_j\right),\end{aligned} \tag{B12}$$

where we have used the last inequality in (B2). Due to (B11) and (B12), we can use

$$\mathbb{E}\left\{U(\boldsymbol{X}(t),t) - U(\boldsymbol{X}(t_0),t_0) - \int_{t_0}^{t}\mathcal{L}U(\boldsymbol{X}(s),s)|^{(32)}ds\right\} = 0, \tag{B13}$$

$\forall t \ge t_0$, where $\mathcal{L}U|^{(32)}$ denotes the infinitesimal generator of U along the solutions of (32), to write (38) as:

$$\begin{aligned}J(\boldsymbol{u}) = \sup_{\mathcal{D}}\Bigg(\lim_{t\to\infty}\sup\mathbb{E}\{2\beta U(\boldsymbol{X}(t_0),t_0) + \int_{t_0}^{t}[2\beta\mathcal{L}U|^{(32)} + \varphi(\boldsymbol{X},\tau) + \beta^2\gamma_2\left(\frac{2}{\beta}\|\boldsymbol{R}_2^{\frac{1}{2}}\boldsymbol{u}\|\right) - \beta\lambda_0\gamma_0\left(\frac{2\|\boldsymbol{\theta}_0\|}{\lambda_0}\right)\\ -\beta\lambda_1\gamma_1\left(\frac{\|\boldsymbol{\Theta}\boldsymbol{\Theta}^T\|}{\lambda_1}\right) - 2\beta\sum_{j=1}^{m_2}\mu_j\gamma_{3j}\left(\frac{1}{\mu_j}\varpi_j\right)]d\tau\}\Bigg).\end{aligned} \tag{B14}$$

Now, with $\varphi(\boldsymbol{X},\tau)$ given in (39) we calculate:

$$\begin{aligned}\Gamma &:= 2\beta\mathcal{L}U|^{(32)} + \varphi(\boldsymbol{X},\tau)\\ &= 2\beta U_{\boldsymbol{X}}\boldsymbol{G}_0\boldsymbol{\theta}_0 + \beta\mathrm{Tr}\left(\boldsymbol{\Theta}_1^T\boldsymbol{G}_1^T U_{\boldsymbol{XX}}\boldsymbol{G}_1\boldsymbol{\Theta}_1\right) + 2\beta\sum_{j=1}^{m_2}[U\left(\boldsymbol{X}+\boldsymbol{\Phi}^{(j)},t\right) - U - U_{\boldsymbol{X}}\boldsymbol{\Phi}^{(j)}]\varpi_j\\ &\quad + 2\beta U_{\boldsymbol{X}}\boldsymbol{G}_2\boldsymbol{u} + \beta^2\ell\gamma_2\left(\|U_{\boldsymbol{X}}\boldsymbol{G}_2\boldsymbol{R}_2^{-\frac{1}{2}}\|\right) - \beta\lambda_0\ell\gamma_0\left(\|U_{\boldsymbol{X}}\boldsymbol{G}_0\|\right) - \beta\lambda_1\ell\gamma_1\left(\|\boldsymbol{G}_1^T U_{\boldsymbol{XX}}\boldsymbol{G}_1\|\right)\\ &\quad - 2\beta\sum_{j=1}^{m_2}\mu_j\ell\gamma_{3j}\left(|U\left(\boldsymbol{X}+\boldsymbol{\Phi}^{(j)},t\right) - U - U_{\boldsymbol{X}}\boldsymbol{\Phi}^{(j)}|\right).\end{aligned} \tag{B15}$$

https://doi.org/10.1017/S0263574721000333 Published online by Cambridge University Press

Let

$$\Gamma^\star := \Gamma + \beta^2\gamma_2\left(\frac{2}{\beta}\|\boldsymbol{R}_2^{\frac{1}{2}}\boldsymbol{u}\|\right) - \beta\lambda_0\gamma_0\left(\frac{2\|\boldsymbol{\theta}_0\|}{\lambda_0}\right) - \beta\lambda_1\gamma_1\left(\frac{\|\boldsymbol{\Theta}_1\boldsymbol{\Theta}_1^T\|}{\lambda_1}\right) - 2\beta\sum_{j=1}^{m_2}\mu_j\gamma_{3j}\left(\frac{1}{\mu_j}\varpi_j\right). \tag{B16}$$

We can write (B14) as

$$J(\boldsymbol{u}) = \sup_{\mathcal{D}}\left(\lim_{t\to\infty}\sup\mathbb{E}\{2\beta U(\boldsymbol{X}(t_0), t_0) + \int_{t_0}^{t}\Gamma^\star d\tau\}\right). \tag{B17}$$

Using the general Young inequality, we have

$$\begin{aligned} -2\beta U_{\boldsymbol{X}}\boldsymbol{G}_2\boldsymbol{u} &= \beta^2\gamma_2'\left(\frac{2}{\beta}\|\boldsymbol{R}_2^{\frac{1}{2}}\boldsymbol{u}^\star\|\right)\frac{\left(\frac{2}{\beta}\boldsymbol{R}_2^{\frac{1}{2}}\boldsymbol{u}^\star\right)^T}{\frac{2}{\beta}\|\boldsymbol{R}_2^{\frac{1}{2}}\boldsymbol{u}^\star\|}\frac{2}{\beta}\boldsymbol{R}^{\frac{1}{2}}\boldsymbol{u} \\ &\le \beta^2\ell\gamma_2\left(\|\gamma_2'\left(\frac{2}{\beta}\|\boldsymbol{R}_2^{\frac{1}{2}}\boldsymbol{u}^\star\|\right)\frac{\left(\frac{2}{\beta}\boldsymbol{R}_2^{\frac{1}{2}}\boldsymbol{u}^\star\right)^T}{\frac{2}{\beta}\|\boldsymbol{R}_2^{\frac{1}{2}}\boldsymbol{u}^\star\|}\|\right) + \beta^2\gamma_2\left(\frac{2}{\beta}\|\boldsymbol{R}^{\frac{1}{2}}\boldsymbol{u}\|\right). \end{aligned} \tag{B18}$$

The equalities of the last inequality in (B18) and (B8) hold if and only if:

$$\begin{aligned} \|\boldsymbol{\theta}_0^*\| &= \frac{\lambda_0}{2}\left(\gamma_0'\right)^{-1}\left(\|U_{\boldsymbol{X}}\boldsymbol{G}_0\|\right)\frac{U_{\boldsymbol{X}}\boldsymbol{G}_0}{\|U_{\boldsymbol{X}}\boldsymbol{G}_0\|}, \\ \left(\boldsymbol{\Theta}_1\boldsymbol{\Theta}_1^T\right)^\star &= \lambda_1\left(\gamma_1'\right)^{-1}\left(\|\boldsymbol{G}_1^T U_{\boldsymbol{X}\boldsymbol{X}}\boldsymbol{G}_1\|\right)\frac{\boldsymbol{G}_1^T U_{\boldsymbol{X}\boldsymbol{X}}\boldsymbol{G}_1}{\|\boldsymbol{G}_1^T U_{\boldsymbol{X}\boldsymbol{X}}\boldsymbol{G}_1\|}, \\ \varpi_j^\star &= \mu_j\left(\gamma_{3j}'\right)^{-1}\left(|U\left(\boldsymbol{X}+\boldsymbol{\Phi}^{(j)}, t\right) - U - U_{\boldsymbol{X}}\boldsymbol{\Phi}^{(j)}|\right)\frac{U\left(\boldsymbol{X}+\boldsymbol{\Phi}^{(j)}, t\right) - U - U_{\boldsymbol{X}}\boldsymbol{\Phi}^{(j)}}{|U\left(\boldsymbol{X}+\boldsymbol{\Phi}^{(j)}, t\right) - U - U_{\boldsymbol{X}}\boldsymbol{\Phi}^{(j)}|}, \\ \gamma_2'\left(\frac{2}{\beta}\|\boldsymbol{R}_2^{\frac{1}{2}}\boldsymbol{u}^\star\|\right)\frac{\left(\frac{2}{\beta}\boldsymbol{R}_2^{\frac{1}{2}}\boldsymbol{u}^\star\right)^T}{\frac{2}{\beta}\|\boldsymbol{R}_2^{\frac{1}{2}}\boldsymbol{u}^\star\|} &= \gamma_2'\left(\frac{2}{\beta}\|\boldsymbol{R}_2^{\frac{1}{2}}\boldsymbol{u}\|\right)\frac{\left(\frac{2}{\beta}\boldsymbol{R}_2^{\frac{1}{2}}\boldsymbol{u}^T\right.}{\frac{2}{\beta}\|\boldsymbol{R}_2^{\frac{1}{2}}\boldsymbol{u}\|}. \end{aligned} \tag{B19}$$

So the "worst case" unknown characteristics are given in the first two equalities in (B19), the minimum of (B17) is reached when $\boldsymbol{u} = \boldsymbol{u}^\star$ as seen from the last equality in (B19), and

$$\min_{\boldsymbol{u}} J(\boldsymbol{u}) = 2\beta\mathbb{E}\left\{U(\boldsymbol{X}_0, t_0)\right\}. \tag{B20}$$

B.4. Proof of continuity and HJI equation (40)

Continuity can be analogously proved as that in the proof of Theorem 3.1 in ref. [43]. The HJI Eq. (40) is directly verified by substituting $\varphi(\boldsymbol{X}, t)$ given in (39) into (40). □

Cite this article: K. D. Do (2021). "Global inverse optimal exponential path-tracking control of mobile robots driven by Lévy processes", Robotica **39**, 2306–2332. https://doi.org/10.1017/S0263574721000333

https://doi.org/10.1017/S0263574721000333 Published online by Cambridge University Press